



ΠΑΝΕΠΙΣΤΗΜΙΟ ΚΡΗΤΗΣ
UNIVERSITY OF CRETE



FORTH

INSTITUTE OF MOLECULAR BIOLOGY & BIOTECHNOLOGY

Graduate Program in Molecular Biology & Biomedicine

Archontidis Themistoklis (AM: 425)

Master Thesis

Development of CRISPR/Cas9-based technologies for genome editing in pancrustacan model organisms

Ανάπτυξη τεχνολογιών CRISPR/Cas9 για τη γονιδιωματική τροποποίηση πανκαρκινοειδών μοντέλων οργανισμών

**Supervisor: Dr. Anastasios Pavlopoulos,
Developmental Morphogenesis Laboratory
IMBB-FORTH**

**Co-supervisors: Prof. John Vontas,
Faculty of Crop Science, Agricultural University of
Athens & IMBB-FORTH**

**Prof. Christos Delidakis,
Department of Biology, University of Crete &
IMBB-FORTH**

Table of Contents:

Ευχαριστίες.....	3
1.1) Περίληψη.....	4
1.2) Summary.....	4
2) General Introduction.....	6
Gene editing technologies: An overview.....	6
CRISPR knock-in approaches and their applications.....	10
3) Part 1: Usage of CRISPR knock in with single stranded oligos (ssODNs) in <i>Tribolium castaneum</i> for the study of phosphine resistance mechanisms	
3.1) Introduction.....	16
Pesticide resistance: An overview.....	16
Phosphine: A widely used pesticide for the control of stored product pests.....	17
<i>Tribolium castaneum</i> : An insect model species for insect molecular biology, evolution and development.....	19
3.2) Results and Discussion.....	22
4) Part 2: Usage of HDR-independent CRISPR knock for the study of vivo activity of UAS/Gal4 binary system variants in <i>Parhyale hawaiiensis</i>	
Introduction.....	31
Binary expression systems: A valuable tool for gene functional analysis.....	31
The binary expression system UAS/Gal4.....	32
<i>Distal-less</i> : A fundamental gene in the development of arthropod appendages.....	35
<i>Parhyale hawaiiensis</i> : An emerging crustacean model species in evolutionary and developmental biology.....	36
Results and Discussion.....	39
Conclusions.....	46
Materials and Methods.....	46
References.....	50

Ευχαριστίες:

Πρώτα από όλα θα ήθελα να ευχαριστήσω τον επιβλέποντά μου, Δρ Αναστάσιο Παυλόπουλο για την ευκαιρία που μου έδωσε να είμαι μέλος της εργαστηριακής του ομάδας κατά τη διάρκεια της μεταπτυχιακού μου, καθώς και για όλη του τη βοήθεια και την υποστήριξη κατά τη διάρκεια αυτού. Επίσης, θα ήθελα να ευχαριστήσω και τα άλλα δύο μέλη της επιτροπής μου, τους καθηγητές Ιωάννη Βόντα και Χρήστο Δελιδάκη για τη συνεισφορά και τη συνεργασία τους κατά τη διάρκεια του μεταπτυχιακού.

Από το εργαστήριο Μοριακής Εντομολογίας και Ελέγχου Παρασίτων, θα ήθελα να ευχαριστήσω τον Δρ Γιώργο Σαμαντσίδα για όλη του τη συνεισφορά και τη καθοδήγηση πάνω στο project για το *Tribolium castaneum*, καθώς και τις Δρ Λίντα Γρηγοράκη, Αμαλία Ανθούση και Σοφία Καφόρου για τη βοήθεια τους κατά τη διάρκεια του ίδιου project.

Επιπλέον, θα ήθελα ευχαριστήσω ιδιαίτερα τη μεταδιδακτορική ερευνήτρια Βάλια Σταματάκη και τη lab manager Μαρίνα Ιωάννου για τη πολύτιμη βοήθεια τους στη πραγματοποίηση όλων των εργαστηριακών πειραμάτων που έγιναν σε αυτή τη μεταπτυχιακή εργασία.

Πάνω στο ίδιο πλαίσιο, θα ήθελα να πω ένα μεγάλο ευχαριστώ στο διδακτορικό Γιάννη Ράλλη, τις μεταπτυχιακές φοιτήτριες Μαρία Καλογερίδη και Νιόβη Ραφαηλίδου και τους προπτυχιακούς φοιτητές Γιάννη Λιάσκα και Εβελίνα Παπαγρηγοράκη για το πολύ όμορφο εργασιακό κλίμα που δημιουργούσαν στο εργαστήριο, καθώς και για όλη τους τη συνεργασία κατά τη διάρκεια αυτού του μεταπτυχιακού. Στους συγκεκριμένους, χρωστάω ιδιαίτερα μεγάλη ευγνωμοσύνη και για όλη τους την υποστήριξη εκτός εργαστηρίου, μαζί με τους: Βάιο Θεοδωσίου, Γεράσιμο Τζιβρά, Αγγελική Σωτηρίου, Teresa Rubio, Μάνο Κόκκα και Βασιλική Καπουλέα. Χωρίς τη πολύτιμη συμπαράσταση αυτών των έντεκα ατόμων, η διεκπεραίωση αυτής τη εργασίας θα ήταν πολύ πιο δύσκολη.

Τέλος, θα ήθελα να πω ένα πάρα πολύ μεγάλο ευχαριστώ στους γονείς μου και την αδερφή μου, Αρχοντίδη Σοφία. Οτιδήποτε έχω καταφέρει μέχρι σήμερα, δεν θα ήταν εφικτό χωρίς τη όλη αυτή την αγάπη και την υποστήριξη που έχουν προσφέρει όλα αυτά τα χρόνια.

1.1 Περίληψη

Το σύστημα γονιδιωματικής τροποποίησης CRISPR/Cas9 αποτελεί μια επαναστατική τεχνολογία που προσφέρει έναν απλό και ακριβή τρόπο για λειτουργικές γενετικές μελέτες σε διάφορα ερευνητικά πεδία της βιολογίας. Η τεχνολογία αυτή είναι ιδιαίτερα σημαντική για μελέτες σε αναδυόμενους οργανισμούς-μοντέλα με περιορισμένα πειραματικά εργαλεία που έχουν να ωφεληθούν πολύ από νέες μεθοδολογίες για την αδρανοποίηση (knockout) και εισαγωγή αλληλουχιών (knock in) σε γονίδια στόχους. Σκοπός της συγκεκριμένης εργασίας ήταν η ανάπτυξη και βελτιστοποίηση διαφορετικών CRISPR/Cas9 knock in τεχνικών σε δύο αναδυόμενα μοντέλα πανκαρκινοειδών: το κολεόπτερο έντομο *Tribolium castaneum* και το αμφίποδο καρκινοειδές *Parhyale hawaiiensis*. Στην περίπτωση του *Tribolium castaneum*, εφαρμόστηκε η τεχνική CRISPR knock in με τη χρήση μικρών μονόκλωνων μορίων DNA (ssODNs) για την εισαγωγή συγκεκριμένων μη συνώνυμων μεταλλάξεων σε δύο γονίδια, τα *dld* και *Cyt-b5-fad*, που έχουν εμπλακεί στην ανθεκτικότητα των εντόμων στη φωσφίνη. Στην περίπτωση του *Parhyale hawaiiensis*, επιλέχτηκε μία στρατηγική CRISPR/Cas9 knock in που βασίζεται σε μη ομόλογο μηχανισμό επιδιόρθωσης (non-homologous end joining) για να ελεγχθεί in vivo το δυαδικό σύστημα γονιδιακής έκφρασης UAS/Gal4. Παρουσιάζονται ποσοτικές και ποιοτικές παράμετροι αυτών των προσεγγίσεων και συζητιούνται για μελλοντικούς πειραματισμούς στα δύο αυτά μοντέλα πανκαρκινοειδών.

1.2 Summary

The Clustered Regularly Interspaced Short Palindromic Repeats (CRISPR) / CRISPR-associated protein 9 (Cas9) genome editing system is a breakthrough technology that provides a simple and accurate way for performing functional genetic analyses in several fields of biological research. This is especially important for studies involving emerging model organisms with limited experimental tools that would benefit greatly from gene knock in and knock out approaches. This project was focused on the development and optimization of different CRISPR/Cas9 knock in strategies on two emerging pancrustacean model species: the coleopteran insect *Tribolium castaneum* and the amphipod crustacean *Parhyale hawaiiensis*. In the case of *Tribolium castaneum*, CRISPR knock in with single stranded oligos (ssODNs) was used in order to introduce specific non synonymous mutations in two genes, *dld* and *Cyt-b5-fad*, which have been implicated in insect resistance to phosphine. In the case of *Parhyale hawaiiensis*, a CRISPR knock in strategy based on the non-homologous end joining repair mechanism was selected to test in vivo the UAS/Gal4 binary system for gene expression. Quantitative and qualitative parameters for both approaches are presented and discussed for future experimentation in these pancrustacean models.

2.General Introduction

Gene editing technologies: An overview

In branches of biology where the need to identify the functional role of specific genes can be a constantly reappearing problem (such as functional genetics and developmental biology), effective gene editing approaches are of utmost importance. This term refers to all the available technologies of genetic engineering that can target and modify genomic sequences in a specific way, in contrary to the random genetic alternation that other technologies do (e.g. random mutagenesis).

In order to accomplish these genetic alternation each gene editing technologies utilize a type nuclease that can recognize and cut specific DNA sequences in vivo, resulting in double stranded breaks (DSBs) (González Castro et al., 2021). The modification is later achieved by the activation of one of the two evolutionary conserved methods of DSBs repair: Non Homologous End Joining (NHEJ) and Homologous Directed Repair (HDR) (González Castro et al., 2021). The first pathway directly ligates the two break ends without requiring a homologous template (Figure 1) (González Castro et al., 2021). For that reason it is prone to errors, due to the possible loss of nucleotides in the site of break and can result in mutations on the repaired genomic sequence (Figure 1) (González Castro et al., 2021). HDR on the other hand, fixes the break only when there is a second homologous sequence available (Figure 1). This ensures an accurate repair of the broken region without any loss of information (Figure 1) (González Castro et al., 2021), however the efficiency of HDR repairs is much lower (González Castro et al., 2021)

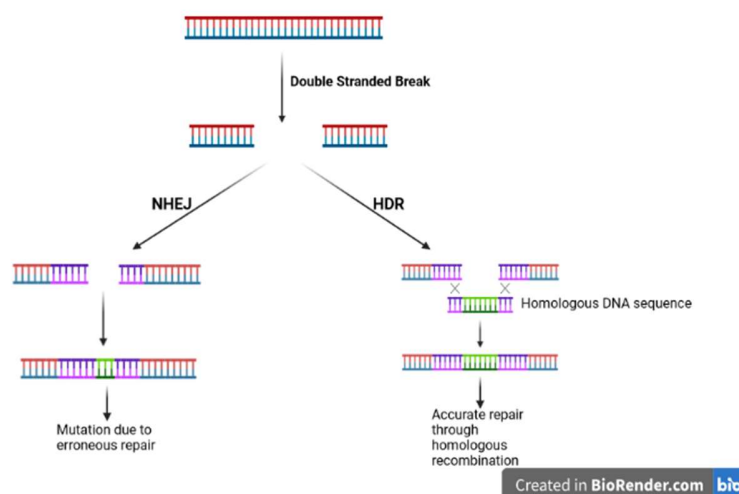


Figure 1: DNA repair mechanisms of double stranded breaks (DSBs). Image created in BioRender.com.

The type of nuclease used by each approach varies, as there was a rapid change in the gene editing technologies over the last decades due to the constant need of more precise and easily applicable methods that are not very costly. The first ones to be used were the meganucleases, a category of restriction enzymes that have very large recognition sequences (generally around 14-40bp) that were observed in a wide range of both prokaryotic (bacteria, archaea) and eukaryotic (fungi, protozoa, algae and plants) organisms, with the later generally found in mitochondrial or plastid genomes (González Castro et al., 2021). Genes encoding such nuclease can be both free standing or be part of introns and inteins (Figure 2)(Arbuthnot, 2015). Whereas the most well know role of restriction enzymes in nature is providing protection against invading DNA, meganucleases functions to help the propagation of the genomic regions that encode them which act as mobile genetic elements (Figure 2) (Arbuthnot, 2015). The movement of those elements starts with the cutting of the host cell's genomic DNA by their meganucleases. However, because the recognition sequences of those endonucleases are quite large, this can be done in a very few specific locations around the genome (Jasin, 1996) (Burt and Koufopanou, 2004). The generated DSBs are later fixed by HDR with the mobile elements acting as homologous templates, resulting in their duplication (Figure 2) (Burt and Koufopanou, 2004). This process is known as homing and for that reason these enzymes are also known as “homing endonucleases” (Arbuthnot, 2015).Both natural and modified meganucleases have been used for gene editing. However, natural ones can target very few specific sequences and the protein engineering required for the creation of modified ones is a very time-consuming process (González Castro et al., 2021).

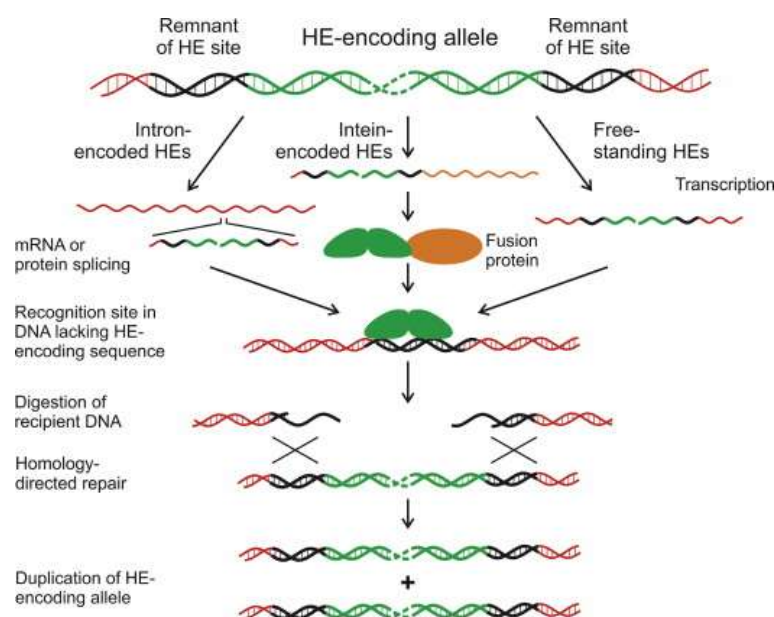


Figure 2: Propagation of homing endonuclease (HE)-encoding genetic elements. Image taken from Arbuthnot, 2015.

The second type of nucleases that appeared in gene editing was the completely artificial zinc finger nucleases (ZFNs). Their structure is made by two different protein domains: an N-terminal region consisting of 3-6 zinc finger motifs (ZFs) and the catalytic domain of FokI in the C-terminal region (Figure 3)(González Castro et al., 2021). ZFs are well known DNA-binding motifs first identified in the transcription factor IIIA (TFIIIA) of *Xenopus laevis* each being 30 amino acids in length and recognizing a

sequence of approximately 3bp, whereas FokI is a type IIS restriction enzyme (which cut DNA at a defined distance from their recognition sequence (Szybalski et al., 1991)) that was isolated from *Flavobacterium okeanokoites* (González Castro et al., 2021). By 3-6ZFs together, an artificial DNA-binding domain can be created which is capable of recognizing a specific sequence of 9-18bp, which can later be fused to the catalytic domain of FokI (Figure 3) (González Castro et al., 2021). However, because ZFNs use the catalytic domain of a type IIS enzyme, they must be in dimeric form in order to be active (Figure 3) (Bitinaite et al., 1998). So, for the targeting of any DNA sequence, two molecules of ZFNs are necessary (Figure 3). Despite being a much more flexible alternative compared to meganucleases, ZFNs also have several problems. The first one is that ZFNs also require great expertise in protein engineering for their designing (González Castro et al., 2021). In addition, the very limited genome accessibility is still not solved in a great depth, as the number of possible target sites for which a ZFN can be created remains quite small (González Castro et al., 2021). On top of that, ZFNs that have DNA-binding domains with more than four zinc finger motifs show reduction in both affinity and specificity which can result in lower stability and higher probability of off-target cleavages (González Castro et al., 2021).

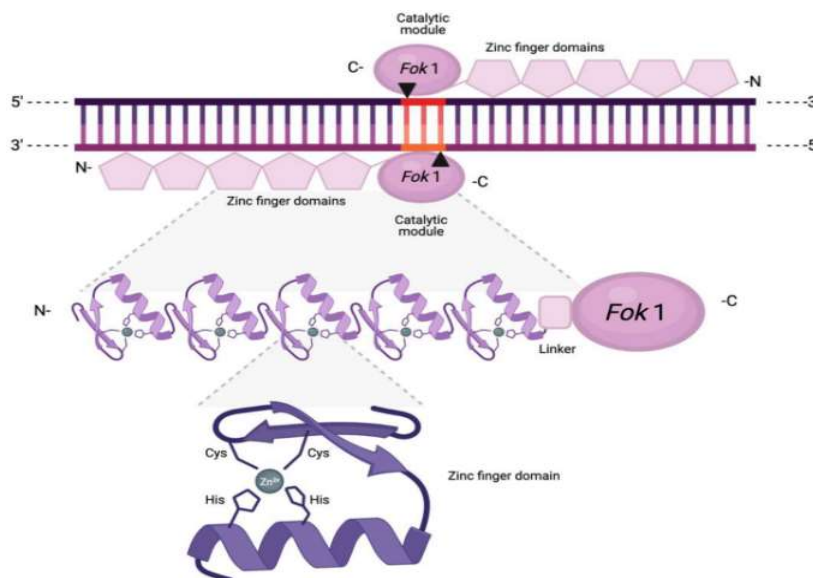


Figure 3: DNA editing with zinc finger nucleases (ZFNs). Image taken from González Castro et al., 2021.

Another type of artificial nucleases, similar to the ZFN technology are the transcription activator-like effector nucleases (TALENs). Their design is similar to that of ZFNs, with the only difference being in the DNA-binding domain which is based on the transcription activator-like effectors (TALEs) (González Castro et al., 2021). These are very small virulence proteins secreted by plant-pathogenic *Xanthomonas* species that bind to specific sequences in the genome of the host plant's cells, in order to activate the expression of genes that alters the plants susceptibility and/or resistance (González Castro et al., 2021), (Zhang et al., 2015), (Ji et al., 2022). The most interesting characteristic of TALEs is that they use a very unique way to recognize their targets sequences, with their DNA-binding domain being composed by a repetition of extremely similar tandem repeats that differ only in two amino acids at positions 12 and 13 (known as repeat variable diresidues or RVDs) (Figure 4) (González Castro et al., 2021). Those

amino acid substitutions are the ones that determine the binding specificity of each repeat, being able to recognize only a specific DNA base (A, T, C or G) (Figure 4) (González Castro et al., 2021). As a result, TALEs bind to their respective sequences using a one-to-one recognition method between a single repeat and a single base (Figure 4) (González Castro et al., 2021). By using these repeats in the place of ZFs, it is possible to create nucleases that can target a much greater array of DNA sequences in a more simplified manner, solving both the genome accessibility problem and the complicated protein design (González Castro et al., 2021).

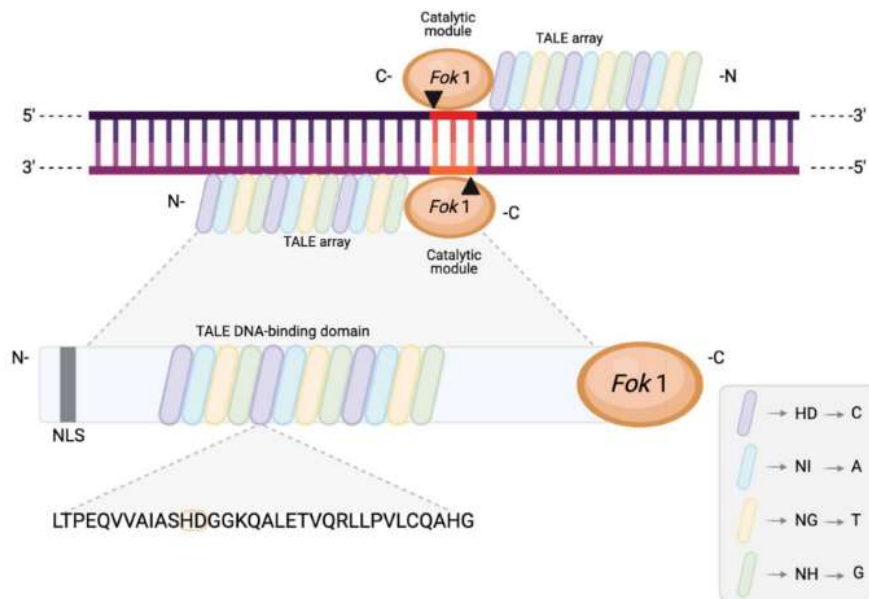


Figure 4: DNA editing with transcription activator-like effector nucleases (TALENs). The small table at the right of the figure presents the different types of RVDs and the nucleotide they recognize. NLS = Nuclear Localization Signal. Image taken from González Castro et al., 2021.

However, it is the emergence of another technology that totally changed the future of gene editing and it is a result of a completely different approach. Genomic analyses conducted in prokaryotic organisms during 1980s and 1990s, discovered the presence of specific regions in their genomes that was composed by a cluster of directed repeats that were interrupted by other non-repetitive DNA sequences (called spacers) (Figure 5A) (Ishino et al., 1987)(van Soolingen et al., 1993)(Mojica et al., 2000). It was later observed, that some of these spacers had identical sequences with ones found on phage genomes and that the addition of new such spacers in the cluster was directly related to the development of resistance against them (Bolotin et al., 2005)(Mojica et al., 2005)(Pourcel et al., 2005)(Barrangou et al., 2007)(Deveau et al., 2008). These genomic parts are known as CRISPR (Clustered Regularly Interspaced Short Palindromic Repeats) and have an extremely important role in bacterial immunity against viral invasion. The cluster acts as storage of sequences obtained from phages that have infected the cell in the past, which can later be transcribed into small RNA molecules (known as crRNA) (Figure 5A) (Brouns et al., 2008). These RNAs form complexes with certain CRISPR-associated nucleases (Cas), acting as complementary templates for the specific targeting and digestion of the viral DNA or RNA from which they were obtained and preventing a second invasion from the same phages (Figure 5A) (Brouns et al.,

2008)(Hale et al., 2009)(Marraffini and Sontheimer, 2008). There are various types of CRISPR systems among the prokaryotes, differing on the mechanisms used for the acquisition and targeting of phage genomic sequences(Hsu et al., 2014). The best studied is probably the type II CRISPR system, which uses a single nuclease called Cas9 (formerly known as Cas5 or Csn1) in order to digest any foreign DNA invading the cell (Figure 5B)(Garneau et al., 2010).The digestion is performed upstream of a very small specific motif (e.g. 5'-NGG-3' for the type II CRISPR system of *Streptococcus pyogenes* (Anders et al., 2014)) called PAM (Protospacer Adjacent Motif) which is found 2-6 nucleotides downstream of the crRNA-targeted sequence (Figure 5B) (Bolotin et al., 2005)(Deveau et al., 2008)(González Castro et al., 2021). One other characteristic of this system is that Cas9 requires the presence of a second trans-encoded small RNA called tracrRNA (Figure 5B) (Deltcheva et al., 2011). However it has been shown that the two RNAs can be fused together in one molecule (the single guide RNA or sgRNA) without any problem, reducing the number of the needed components(Jinek et al., 2012). So, by using the Cas9 protein in combination with an artificial sgRNA that can recognize a specific genomic site it is possible to perform gene editing in an extremely simple and effective way. This is because there is no need for complex protein engineering in this approach, with a single nuclease being able to target any genomic sequence if paired with a complementary sgRNA(Hsu et al., 2014)(González Castro et al., 2021). As a result, the use of the CRISPR/Cas9 system has rendered genomic modification in different organisms easier and more accurate than ever before.

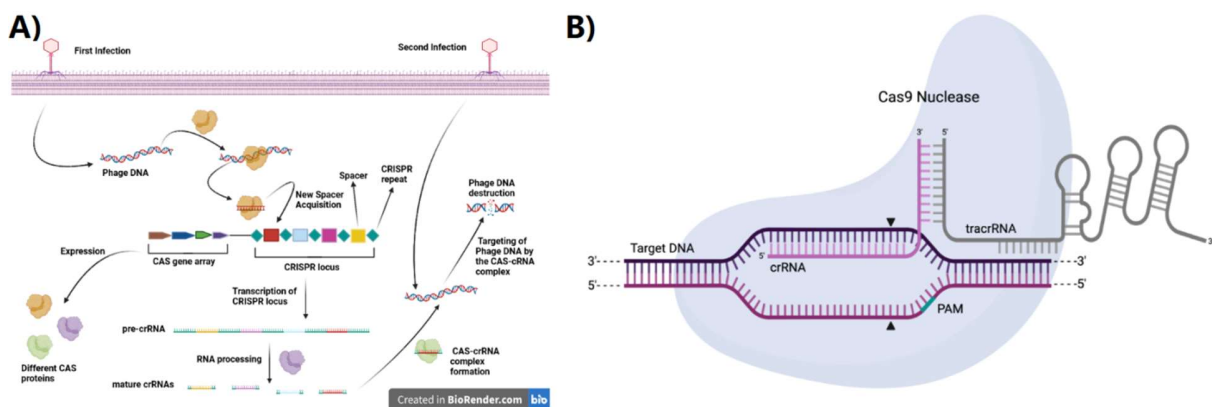


Figure 5: (A) General Mechanism of CRISPR immunity. The acronym CAS refers to CRISPR associated proteins, (B) Structure and DNA binding of the Cas9/crRNA/tracrRNA ribonucleoprotein complex. (A) was created in BioRender.com, whereas (B) was taken from González Castro et al., 2021.

CRISPR knock-in approaches and their applications

As it was described earlier, site specific targeting and alteration of genomic sequences is the defining characteristic of all gene editing technologies. The type of change can be variable and can include deletion, inversion or replacement of different genetic loci, as well as targeted insertion of desired DNA sequences in specific genomic sites. The last category, also known as knock-in, is one of the two fundamental experimental approaches available for the functional analysis of a gene (the other is the targeted inactivation of a gene by the disruption of its correct expression which is known as knock-out).

Knock-in approaches have been diversified and improved greatly with the progress of gene editing. This section will be focused in those based on the CRISPR/Cas9 technology.

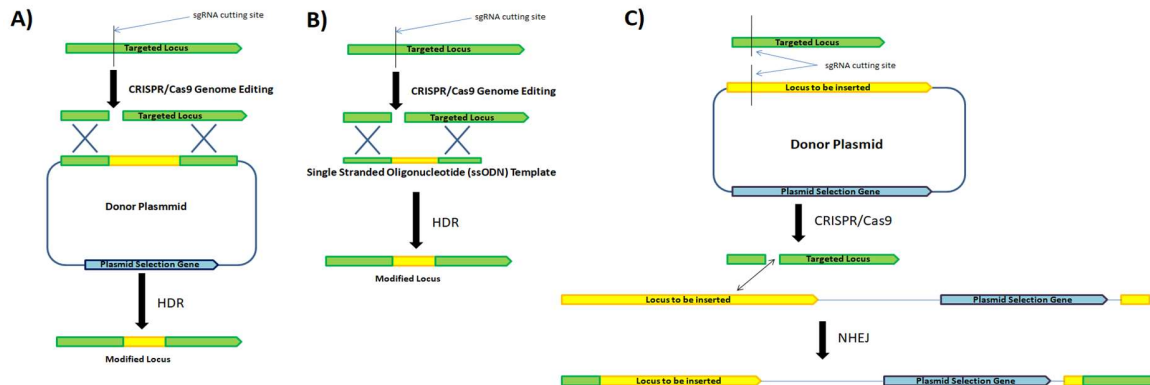


Figure 6: CRISPR knock in approaches that involve: (A) HDR-dependent insertion with plasmid template, (B) HDR-dependent insertion with ssODN template and (C) HDR-independent insertion with NHEJ.

The most common category of CRISPR knock-in is the one that uses the HDR pathway in order to achieve a successful insertion. This is done by adding a DNA molecule to act as a donor and provide the template sequence needed for the homologous repair (Figure 6) (Denes et al., 2021). The nature of this DNA molecule can vary depending on the experiment, with both plasmid donors (Figure 6A) (Gratz et al., 2015)(Denes et al., 2021) or PCR amplified fragments being used (Denes et al., 2021)(Irion et al., 2014). These plasmids contain the sequence to be inserted flanked by two homologous arms (sequences that have high homology with the genomic regions around the target site) (Figure 6A) (Denes et al., 2021). The size of homologous arms in plasmid donors are generally around 0.5-2kb (Denes et al., 2021). Usually, marker genes are also added in the template for easy phenotypic screening of the knock-in events (Gratz et al., 2015). The advantage of this method is that it allows the insertion of very large DNA fragments (>1kb), although increasing the length of the inserted sequence reduces the efficiency of knock-in (Denes et al., 2021). It has been successfully accomplished in different model organisms (e.g. *Drosophila melanogaster* (Gratz et al., 2014), *Tribolium castaneum* (Gilles et al., 2015) and *Danio rerio* (Irion et al., 2014)).

However, the use of plasmid donors for HDR-based knock-in is limited to well-characterized genomic regions around the target site. The reason for this is that the required homologous arms are very large and their design can be problematic when there is limited sequence availability for a specific locus. This is especially a problem in situations where the studied organism doesn't have its whole genome sequenced or if the available genomic sequence is not very well annotated. In these conditions, the use of single stranded oligonucleotides (ssODNs) as donors can provide a solution as they are much smaller in size (60-200 nucleotides) and their homologous arms can be as short as 30 nucleotides each (Figure 6B) (Denes et al., 2021)(Gratz et al., 2015)(Boel et al., 2018). This approach is also quite quicker, as the ssODNs can be rapidly synthesized compared to plasmid donors that require extensive cloning in order to be created (Gratz et al., 2015). However, their small size can also be a limiting factor as they are not a

good choice when large DNA fragments need to be inserted (Gratz et al., 2015). For the same reason, it is very difficult to add marker genes in their sequence and the identification of knock-in animals has to be done by genotyping which is a much more time-consuming process (Gratz et al., 2015). Attempts have been made in order to overcome this problem, by trying to extend the maximum length of the used ssODN (Quadros et al., 2017). The application of this type of knock-in has been performed in a wide variety of different organisms including both invertebrates, such as *Drosophila melanogaster* (Levi et al., 2020), *Ceratitis capitata* (Aumann et al., 2018), *Tribolium castaneum* (Shirai et al., 2022), *Spodoptera exigua* (Zuo et al., 2017) and *Plodia interpunctella* (Heryanto et al., 2022), and vertebrates, such as the teleost *Danio rerio* (Hwang et al., 2013) (Armstrong et al., 2016). In this last organism, a research group (Boel et al., 2018) performed a detailed study in order to test the efficacy of different ssODN designs for the same target sites. More specifically, the group used ssODNs of different size (60 nucleotides, 120 nucleotides and 180 nucleotides), symmetry (with homologous arms of equal or unequal length) and complementarity for the performance of CRISPR knock-in on four different genes (Boel et al., 2018). The conclusion was that the most influential factor of the three was the ssODNs size (with 120 nucleotides being the optimal), whereas symmetry and complementarity didn't have any significant change in the knock-in efficiency (Boel et al., 2018).

CRISPR knock-in that depends on the HDR pathway is maybe the most widely used approach, although there are conditions where its application can be quite problematic. One of the most distinguishing examples is maybe when the available populations of the studied organisms have very high heterozygosity and are rich in genetic polymorphisms, such as the amphipod crustacean *Parhyale hawaiiensis* (Kao et al., 2016). In those circumstances, the designing of homologous arms can be rather troublesome, and so an HDR independent type of knock-in is probably a better option (Kao et al., 2016). This kind of knock-in depends on the NHEJ pathway and the insertion of the desired fragment is achieved by the direct ligation of the cleaved chromosomal and plasmid templates (Figure 6C). The targeted genomic region and the plasmid are linearized at specific positions by the Cas9 protein using either one sgRNA that recognizes both templates or two different sgRNAs (Figure 6C) (Kao et al., 2016) (Bosch et al., 2020). These plasmids, unlike the ones used for the HDR approach, have the extra advantage that can be generally used as inserts in any targeted genomic sequence, as they lack specified homologous arms (Bosch et al., 2020). However, HDR independent knock-in also has disadvantages, the main one being its higher probability for imprecise knock-in events due to the errorprone nature of NHEJ pathway that can result in unwanted indels in the targeted region (Bosch et al., 2020). This method has resulted in successful knock in event in *Parhyale hawaiiensis* (Kao et al., 2016) and has been proposed as a more quick and simple alternative for knock-in in *Drosophila melanogaster* (Bosch et al., 2020). It has been also applied in the teleosts *Danio rerio* (Auer et al., 2014) and *Oryzias latipes* (Watakabe et al., 2018) and in another crustacean species, the cladoceran *Daphnia magna* (Kumagai et al., 2017).

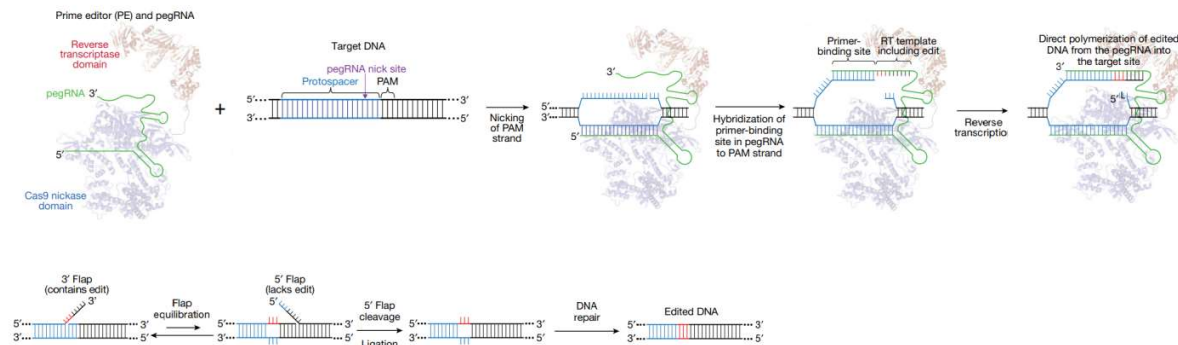


Figure 7:Methodology of gene editing with prime editing. Image taken and edited from Anzalone et al., 2019

Finally, there is a recently developed technique of CRISPR knock in that works by directly rewriting the DNA sequence at the targeted genomic sites (Anzalone et al., 2019)(Smirnikhina, 2020). This approach is called prime editing and uses a very unique way of knock-in strategy. In more detail, this method uses a fusion protein (called the Prime Editor or PE) consisting of a Cas9 H840A nickase and a reverse transcriptase (RT) derived from the Moloney Murine Leukemia Virus (M-MLV) (Figure 7) (Anzalone et al., 2019)(Smirnikhina, 2020). Nickases are catalytically impaired versions of Cas9 that are only able to perform single strand breaks (SSBs)(Trevino and Zhang, 2014). There are different types of nickases that introduce SSBs specifically in one of two strands of the DNA (for example D10A nickase introducing SSBs only in the strand bearing the recognizing sequence, whereas nickases H840A and N863A cut only the opposite one)(Trevino and Zhang, 2014). A special type of sgRNA is also required for this process (called prime editing RNA or pegRNA) which has an extended 3' end that carries the template sequence and a primer binding site (PBS) (Figure 7) (Anzalone et al., 2019)(Smirnikhina, 2020). When this ribonucleoprotein complex binds to its intended genomic site, it nicks the opposite DNA strand creating one 5' phosphate end and one 3' hydroxyl end (Figure 7) (Anzalone et al., 2019). The last one hybridizes with the PBS of the pegRNA, allowing the RT to start the reverse transcription of the template (Anzalone et al., 2019). After the completion of the reaction, an intermediate DNA structure is created which can have two possible forms: one with a 3' flap bearing the desired modified sequence and one with a 5' flap bearing the unwanted original one (Figure 7) (Anzalone et al., 2019). The 3' flap form is probably the most thermodynamically favored of the two (as the hybridization of the complementary 5' flap is expected to be stronger), although free 5' DNA ends are the preferable substrates for the endo- and exonucleases of the repair mechanism (such as FEN1 and EXO1) (Figure 7) (Anzalone et al., 2019). This leads to a preferential digest of the 5' flaps and the creation of a heteroduplex in the site with one edited and one unedited strand (Anzalone et al., 2019). This state activates the mismatch repair pathway (MMR) which can either result in the permanent alteration of target sequence (Figure 7) or the reversion of the edit back to the original form (Anzalone et al., 2019). One way to preserve the edited form is to add an extra sgRNA in the mix that targets only the modified sequence (Figure 8). This results in the nicking of the heteroduplex in the unedited strand, causing its preferential repair over the edited one (Figure 8) (Anzalone et al., 2019). Also, transient impairment of the MMR through the addition of plasmids encoding dominant negative forms of the MLH1 protein (an important component of this pathway) has been shown to improve the efficiency of prime editing (Chen et al., 2021).

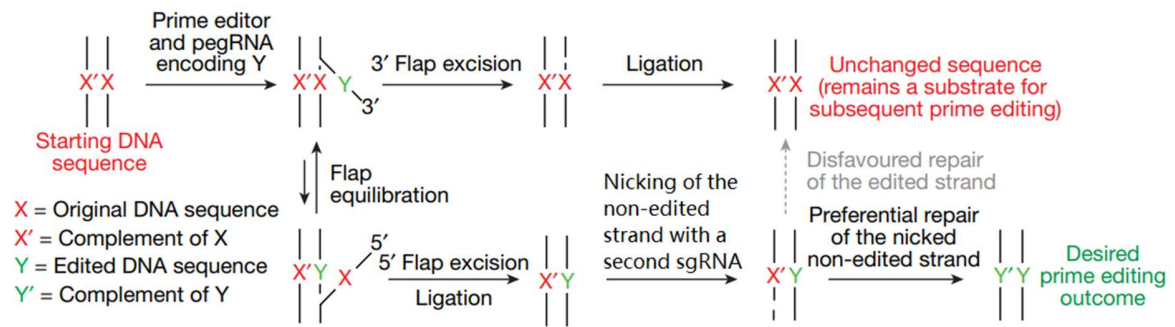


Figure 8: Improved method of prime editing that uses a second sgRNA to digest the non-edited strand of the generated heteroduplex, in order to increase the chances for successful modification of the targeted sequence. Image taken and edited from Anzalone et al., 2019

3. CRISPR knock in with single stranded oligos in Tribolium castaneum for the study of phosphine resistance mechanisms

3.1 Introduction

Pesticide resistance: An overview

Chemical control is the predominant method used today for the control of harmful insects (agricultural pests and disease vectors) and is based on the use of specific chemical compounds with pesticidal activity. However, the long-term overuse of pesticides has increased the proportion of less susceptible individuals in populations of different species.

This phenomenon is the result of selective pressure acting on pest populations. More specifically, in a pest population both resistant and susceptible genotypes are present among its members (Figure 9)(Feyereisen, 1995). However, when there is continuous presence of a pesticide in the environment the resistant genotypes have better survivability and therefore greater reproductive success (Figure 9)(Feyereisen, 1995). As a result, with each generation the frequency of the resistant genotypes increases and the pesticide efficacy drops (Feyereisen, 1995)(Figure 9).

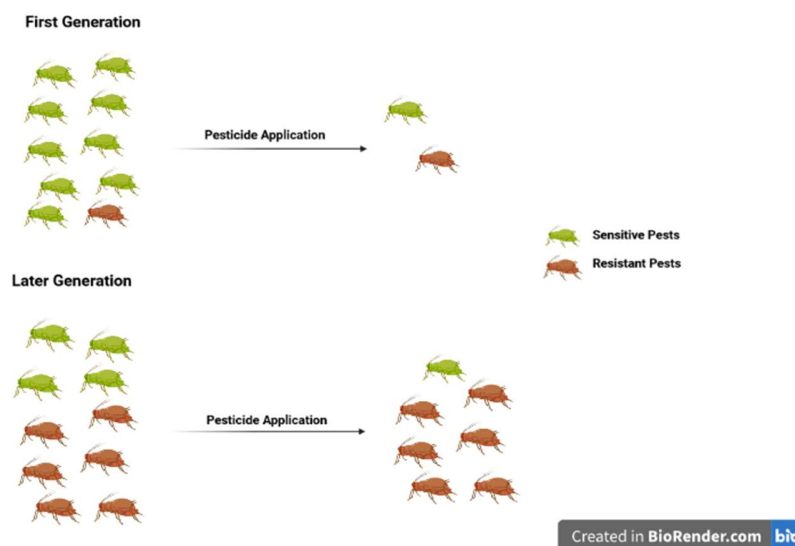


Figure 9: Pesticide resistance emergence into pest populations. Created in BioRender.com.

The molecular mechanisms behind this resistance can involve changes in the proteins targeted by the pesticides, as well as the amplification or overexpression of genes that encode proteins that neutralize the effects of insecticides (Feyereisen, 1995). The first category is maybe the most recognizable, in which the presence of point mutations in the binding sites of the protein-targets reduce their affinity with pesticide (Figure 10A)(Feyereisen, 1995). The second one mainly involves detoxification enzymes that metabolize the pesticides into less harmful forms (Figure 10B)(Feyereisen, 1995). Enzymes of this category include P450 monooxygenases and glutathione S-transferases, both of which act by transferring more polar functional groups to their substrates to produce more polar products that are more extractable and less toxic(Nauen et al., 2022)(Pavlidis et al., 2018). Esterases are also an important type of detoxification enzymes as they catalyze the hydrolysis of ester bonds, which are present in a wide

range of pesticides (Montella et al., 2012). Another group of proteins with important detoxification role is the ABC (ATP-binding cassette) transporters, which actively pump a variety of chemicals across cell membranes, thus, preventing possible toxic compounds to reach their targets (Figure 10B) (Wu et al., 2019). One final mechanism is the reduced pesticide absorption by the pest's body. This specific category mainly involves cuticular resistance in which the thickness of cuticle is increased (by its enrichment in chitin, cuticular hydrocarbons and proteins), making its penetration by the pesticide much more difficult (Figure 10C) (Balabanidou et al., 2018) (Adams et al., 2021).

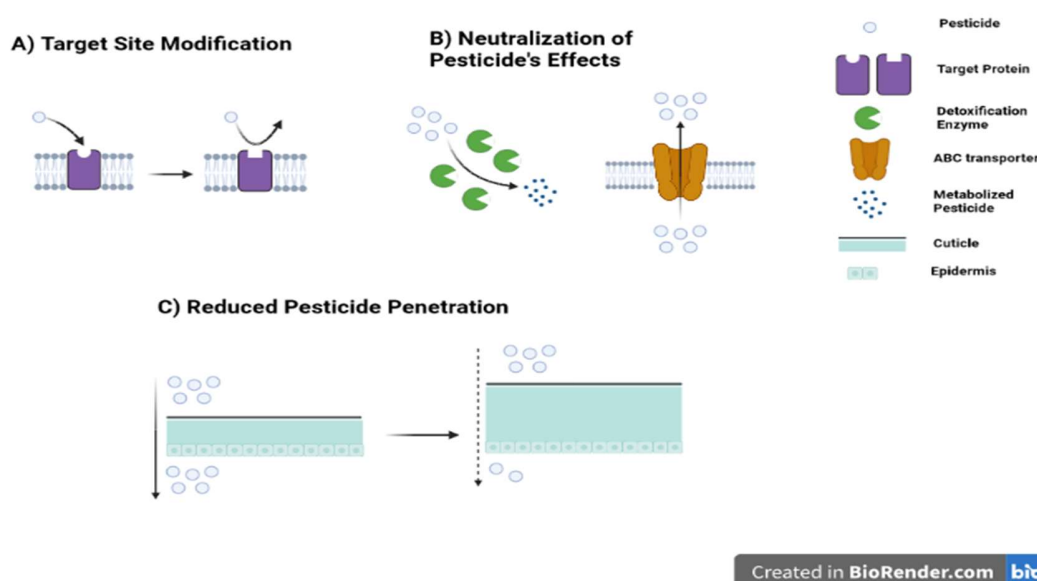


Figure 10: Mechanisms of pesticide resistance. Created in BioRender.com.

Phosphine: A widely used pesticide for the control of stored product pests

The prevalent method used for the prevention of pest infestations on stored products (such as grains or processed foods) facilities is that of fumigation. It involves the dispersion of gaseous pesticides (known as fumigants) in a tightly sealed area in order to exterminate the pests within.

Maybe the most distinguishing pesticide of that category is phosphine (PH_3). Its application as a fumigant begun in 1930s and still remains extremely popular due to its low cost, easy application and absence of residues in the products (Schlipalius et al., 2002). On top of that, its popularity greatly increased after the 1990s when the use of methyl bromide, another widely applied fumigant, was progressively phased out due to its recognition as an ozone-depleting chemical (Schlipalius et al., 2002).

The phosphine fumigation process is generally done by the dispersal of aluminum phosphide (AIP) tablets in the infested areas (Bell, 2014) (Annis et al., 2016). This compound reacts with the atmospheric moisture to generate phosphine gas and aluminum hydroxide ($\text{AlP} + 3 \text{H}_2\text{O} \rightarrow \text{Al}(\text{OH})_3 + \text{PH}_3$) (Bell, 2014) (Annis et al., 2016). In order to minimize the risk of spontaneous combustion (due to phosphine's high flammability) ammonium carbamate ($[\text{NH}_4][\text{H}_2\text{NCO}_2]$) is added to the tablets (Bell, 2014) (Annis et

al, 2016). This compound slowly decomposes at room temperature to release carbon dioxide and ammonia ($[\text{NH}_4][\text{H}_2\text{NCO}_2] \rightleftharpoons 2\text{NH}_3 + \text{CO}_2$), which dilute the released phosphine gas in the air and thus making then conditions much less favorable for self-ignition to occur (Bell, 2014)(Annis et al, 2016). Alternatively, phosphine can be purchased directly as a pressurized gas mixed with nitrogen or carbon dioxide (again for flammability reasons)(Bell, 2014).

However, despite its wide usage all these decades, the mechanism behind the pesticidal action of phosphine is still not very well understood. Accumulated data indicate that the most affected cellular functions by this specific pesticide are the ones that are related with mitochondria and energy metabolism (Nath et al., 2011). This hypothesis is greatly supported by recent observations that mutations in two genes that are related to mitochondrial function, *dld* and *Cyt-b5-fad*, are responsible for the majority of phosphine resistance in several species of stored product pests, including *Tribolium castaneum* (Jagadeesan et al., 2012)(Schlipalius et al., 2018)(Kaur et al., 2015), *Rhyzopertha dominica* (Schlipalius et al., 2002)(Schlipalius et al., 2008)(Schlipalius et al., 2018), *Sitophilus oryzae* (Nguyen et al., 2016)(Schlipalius et al., 2018) and *Cryptolestes ferrugineus* (Jagadeesan et al., 2016)(Schlipalius et al., 2018)(Jagadeesan et al., 2021).

The first of these two genes encodes a protein named dihydrolipoamide dehydrogenase (DLD), an enzyme with vital role in energy metabolism (Carothers et al., 1989)(Schlipalius et al., 2012). It exists as a homodimer and is important component of four crucial mitochondrial multienzyme complexes: pyruvate dehydrogenase, α -ketoglutarate dehydrogenase, branched-chain α -keto acid dehydrogenase and the glycine cleavage system (Carothers et al., 1989)(Schlipalius et al., 2012). The first three complexes are fundamental for the citric acid cycle (an essential metabolic pathway for aerobic energy production), whereas the last one prevents the glycine concentration in body fluids to reach toxic levels (Berg et al., 2015)(Kikuchi et al., 2008). In all these complexes, DLD is responsible for the oxidation of dihydrolipoamide to lipoamide, an essential cofactor for their enzymatic functions (Carothers et al., 1989). Results from genetic screens show that phosphine probably binds to the disulfide catalytic center of the DLD enzyme (as the point mutations that generated phosphine resistant phenotypes in the different pest species and in *Caenorhabditis elegans* where mainly observed around this region), blocking its activity (Schlipalius et al., 2012).

The other gene encodes another enzyme with desaturase activity, adding double bonds into long-chain fatty acids (Schlipalius et al., 2018). Although the exact role of this enzyme in phosphine resistance isn't clear yet, a possible mechanism has been proposed recently (Schlipalius et al., 2018). Several studies have shown that phosphine exposure leads to increased oxidative stress in the cells due to the accumulation of reactive oxygen species (ROS) (Bolter and Chefurka, 1990)(Liu et al., 2015). One of the main types of cellular damage observed in such situations is the destruction of lipids due to fatty acid peroxidation (Chaudhry and Price, 1992)(Valmas et al., 2008)(Liu et al., 2015)(Niu et al., 2013). End products of this process are 4-hydroxynonenal (4-HNE) and malondialdehyde (MDA), both of which are very well known markers of oxidative stress (Chaudhry and Price, 1992). However, molecules like these can cause further damage by affecting a wide variety of reactions involved in cellular respiration(Kaplan et al., 2007). 4-HNE for example is an inhibitor of a wide variety of enzyme complexes due to its very strong affinity for thiol groups, like the ones found in cysteine residues (Carini et al., 2004), such as

complex IV (a fundamental component of the oxidative phosphorylation pathway) (Kaplan et al., 2007). Therefore, mutations that suppress the activity of such desaturases result in a decreased presence of polyunsaturated fatty acids in the cell membranes, limiting the destruction caused by lipid peroxidation (Schlipalius et al., 2018).

One other interesting finding from early studies (when the identity of those genes was still unknown) is that the combined presence of resistant alleles in both genes results in much higher levels of resistance compared to those conferred by each one alone (Schlipalius et al., 2002). This means that they have a synergistic effect on phosphine resistance (Schlipalius et al., 2002). A possible explanation for this is that it is a combined disruption of a synergistic toxicity mechanism that takes place when there is full susceptibility to phosphine (Schlipalius et al., 2018). This is supported by the fact that 4-HNE can also bind very strong to dihydrolipoamide (as it also has thiol groups), inhibiting the electron transfer to the active site of DLD molecules (Humphries and Szweda 1998a)(Humphries and Szweda, 1998b). In those conditions, DLD catalyzes the production of more ROS, leading to further lipid peroxidation and thus repeating the damaging cycle (Schlipalius et al., 2018).

***Tribolium castaneum*: An insect model species for insect molecular biology, evolution and development**

The red flour beetle *Tribolium castaneum* is a coleopteran insect and one of the best known pests of stored grain and flour products. It is also one of best studied insect model species in biological research used in a wide range of subject areas.

T. castaneum was first used for laboratory work around the late 1920s, when Royal N. Chapman used it for studies on population ecology. This was the beginning of its widespread application as a model to address fundamental questions in evolutionary biology and ecology, such as sexual selection, interspecies competition, population regulation and reproductive isolation (Aditi Pai and Gregor Bucher 2019).

Being a holometabolous insect, it undergoes complete metamorphosis during its life cycle which is relatively fast, lasting only 23 days on 32°C (Figure 11A) (Klingler and Bucher, 2022)(Aditi Pai and Gregor Bucher 2019). The embryogenesis is also short and lasts 3 days at 32°C (Figure 11A). When the first instar larvae emerge from the eggs, they go through seven successive larval moults (although the actual number may vary a little depending on food availability) before they are ready to pupate. Larval development takes about 15 days at 32°C (Figure 11A) (Klingler and Bucher, 2022)(Aditi Pai and Gregor Bucher 2019). The metamorphosis completes in 5 days after pupation at 32°C after which they undergo their last molt to finally reach the imago stage (Figure 11A) (Klingler and Bucher, 2022)(Aditi Pai and Gregor Bucher 2019). Sex distinction is much more difficult compared to other insect model species (like *Drosophila*) and it is generally done at the pupal stage with the observation of genital papillae, which are larger in females and bear two pointy tips (Figure 11B) (Brown et al., 2009)(Shukla and Palli, 2012). If needed, sex can be distinguished at the imago stage as the males have two small sex patches at the ventral side of the femur in the first pair of legs (Figure 11B) (Brown et al., 2009)(Shukla and Palli, 2012).

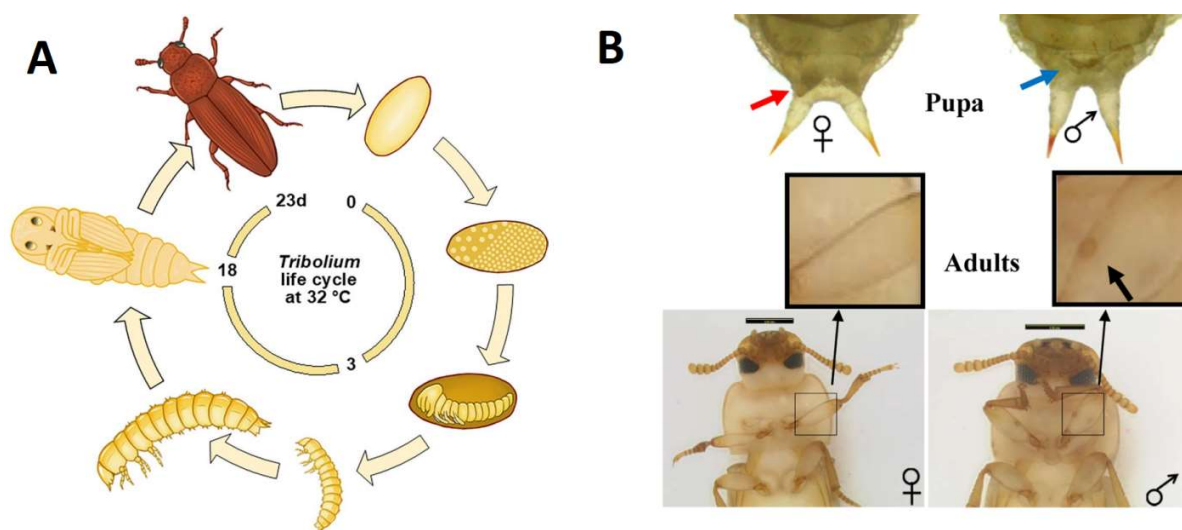


Figure 11: (A) Life cycle of *Tribolium castaneum* at 32°C (only 2 out of the 7 larval stages are depicted). **(B)** Sex determination in the pupal and adult stages of *Tribolium castaneum*. **(A)** was taken from Klingler and Bucher, 2022, whereas **(B)** was taken and modified from Shukla and Palli, 2012.

Since 1960s, *T. castaneum* became an increasingly popular choice for functional genetics approaches and an important model species in arthropod and insect molecular biology (Aditi Pai and Gregor Bucher 2019). The reasons behind this widespread use in these fields were not only limited to its favorable characteristics in rearing (rapid growth, easy maintenance and high fecundity), but also the efficient genetic manipulation with an increasing number of molecular tools (Aditi Pai and Gregor Bucher 2019)(Campbell et al., 2022).

Maybe the most efficient of those tools in *T. castaneum* is RNA interference, as all cells in all tissues can absorb dsRNA from the hemolymph (although this high efficiency is observed only if the dsRNA is longer than 60bp) (Aditi Pai and Gregor Bucher 2019)(Brown et al., 2009)(Klingler and Bucher, 2022). As a result, systemic RNAi experiments can be induced at any desired stage, something that is very useful when the research involves genes that have both early and late functions during the life cycle of the beetle (e.g. leg patterning genes which are active in both the embryonic and the pupal stage)(Aditi Pai and Gregor Bucher 2019)(Brown et al., 2009)(Klingler and Bucher, 2022). Parental RNAi also has very high efficiency in the *T. castaneum*, allowing knock down screens in hundreds of embryos with the injection of a small number of female pupae or adults (Aditi Pai and Gregor Bucher 2019)(Brown et al., 2009)(Klingler and Bucher, 2022). The systemic RNAi response in this species is immensely powerful, with the knock down effects being identical to those observed in null mutants (Aditi Pai and Gregor Bucher 2019)(Brown et al., 2009)(Klingler and Bucher, 2022). However, RNAi is not the only effective molecular tool in *T. castaneum*. Transgenesis with the use of transposons (such as piggyback (Lorenzen et al., 2003) and Minos (Pavlopoulos et al., 2004)) and CRISPR/Cas9 genome editing (Gilles et al., 2015) are also efficient and have been used to create a large number of different genetically modified strains. For all these reasons, *T. castaneum* is the second best studied insect genetic model after *Drosophila melanogaster*. Moreover, since *T. castaneum* is a notorious pest of stored products, it is an

attractive and powerful model for research in pest control(Brown et al., 2009)(Rösner et al., 2020). It has been used in numerous studies to decipher the effects of different pesticides in insect physiology as well as the mechanisms responsible for insecticide resistance (Brown et al., 2009)(Rösner et al., 2020).

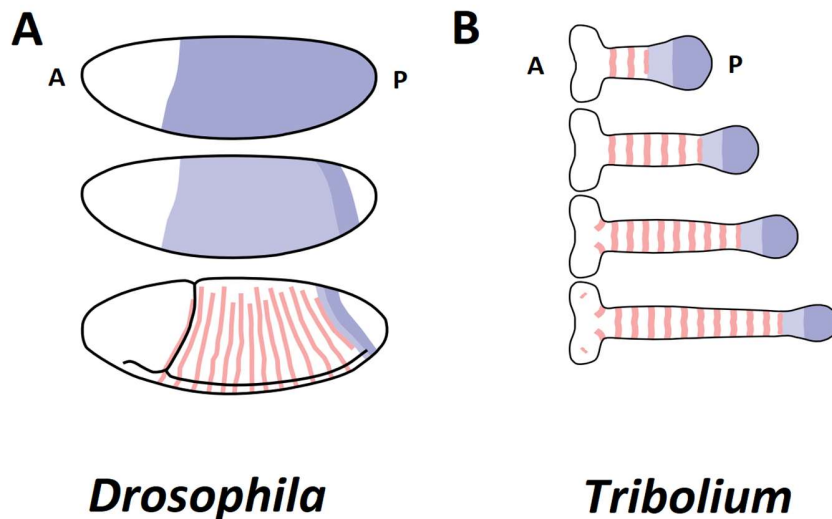


Figure 12: Segmentation in *Drosophila* (A) and *Tribolium* (B). The pink colored stripes represent the formed segments, whereas the blue regions indicate the Segment Addition Zone (SAZ) in *Tribolium* and gap gene expression in *Drosophila*. A-P symbols indicate the anterior-posterior axis. Image taken and modified from Clark et al., 2019.

T.castaneum presents some specific characteristics during its embryogenesis that make it suitable for comparative developmental studies with *Drosophila melanogaster* (Schröder et al., 2008). Many aspects of *Drosophila* embryonic development are evolutionary innovations that are not observed in the vast majority of insects (Schmidt-Ott and Lynch, 2016) (Schröder et al., 2008). In contrast, *T.castaneum* is less derived and a better representative of insect development suitable for comparative and evolutionary studies (Schröder et al., 2008).

One such prominent example that shows these developmental differences between *Drosophila* and *Tribolium* can be seen in the segmentation mechanisms. In *Drosophila*, all the body segments are formed almost simultaneously during the blastoderm stage by the effects of the gap gene network (Figure 12A) (Schmidt-Ott and Lynch, 2016) (Schröder et al., 2008). This so-called long germ mode of segment formation is observed only in holometabolous insect orders (Diptera, Hymenoptera, Lepidoptera and Coleoptera) and is considered a derived evolutionary characteristic (Stern, 2004) (Schmidt-Ott and Lynch, 2016). On the other hand, *Tribolium* exhibits a different kind of segmentation, known as short germ, in which most of the trunk segments are generated after the blastoderm stage where only the cephalic and thoracic segments are specified (Figure 12B) (Schröder et al., 2008). New segments are added sequentially after gastrulation with a clock-like mechanism from a segment addition zone (SAZ) at the posterior end of the embryo (Figure 12B) (Schröder et al., 2008) (Clark et al., 2019).

3.1 Results and Discussion

This part of the thesis was focused on the creation of *dld* and *Cyt-b5-fad* mutant lines of *Tribolium castaneum* in order to test their role in phosphine resistance. More specifically, two screening experiments on different natural resistant *T.castaneum* populations have identified two amino acid substitutions in the products of these genes that were not observed in the sensitive ones: that of proline 45 into serine (P45S) in the case *dld* and that of serine 349 into glycine (S349G) in the case of *Cyt-b5-fad*(Kaur et al., 2015)(Schlipalius et al., 2018). Generating both single and double mutant lines for these two loci would allow the quantitative measurement of the resistance provided by these mutations alone or in combination. Surprisingly, genotyping of the two loci in the laboratory strain *vermillion*^{white} used in these experiments (performed by Mantha Lamprousi in the Vontas group) showed that it was carrying the resistant allele of the *Cyt-b5-fad* locus (Figure 13). Therefore, my goal was to create a line having the sensitive alleles for both genes (by reversing the *Cyt-b5-fad* resistant mutation), one line bearing the resistant *dld* allele and one line having the resistant alleles for both genes (Figure 13).

Line	<i>dld</i>	<i>Cyt-b5-fad</i>	
1 <i>vermillion</i> ^{white} (starting line)	P45 (S)	S349 (R)	<i>dld</i> sensitive <i>Cyt-b5-fad</i> resistant
2	P45 (S)	G349 (S)	<i>dld</i>sensitive <i>Cyt-b5-fad</i> sensitive
3	S45 (R)	S349 (S)	<i>dld</i>resistant <i>Cyt-b5-fad</i>sensitive
4	S45 (R)	G349 (R)	<i>dld</i>resistant <i>Cyt-b5-fad</i>resistant

Figure 13: Overview of the four *T.castaneum* lines and their respective non-synonymous substitution in the *dld* and *Cytb-5-fad* loci. R and S symbols indicate the phosphine resistant and sensitive genotypes for each of the two loci.

Currently, the only established method for CRISPR knock in in *T.castaneum* uses plasmids donors designed for HDR. However, this method is not applicable in our case. Both the *dld* and *Cyt-b5-fad* sequences in the beetle genome are incomplete hampering the design of large homologous arms. As an alternative, the use of ssODNs as templates was selected to generate the desired lines.

The designing of the two ssODNs as well as the sgRNAs needed for the targeting of the loci was done by Dr. George Samantsidis in the Vontas lab. Each ssODN was 200 nucleotides long with about 100 nucleotide homologous arms on either side of the nucleotides targeted for substitution. Each ssODN

carried in the center the nucleotides encoding the desired non synonymous amino acid substitution (P45S for *dld* and G349S for *Cyt-b5-fad*) together with other synonymous substitutions that introduced new restriction sites (Clal in the case of *dld* and BamHI in the case of *Cyt-b5-fad*) for genotyping purposes by Restriction fragment length polymorphism (RFLP) (Figure 14). Extra synonymous mutations were introduced in each ssODN in the PAM and spacer sequences to prevent the recutting of the modified sequence by the Cas9/sgrRNA complex (Figure 14). Finally, one more non synonymous mutation for the reversion of asparagine 358 back to histidine (N358H) was added in the ssODN designed for the *Cyt-b5-fad* gene (Figure 14). This substitution was detected along with S349S in the *T.castaneum* resistant populations in the original study performed by Schlipalius et al., 2018, although later SIFT (Sorting Intolerant From Tolerant) analysis conducted by the group didn't indicated any significant effect in the function of the protein. Regardless of its apparent neutrality, this extra non synonymous substitution was included for comparison with these older studies.

***dld* gene**

```
>>dld/Vermillion (P45)
gtcactcgataatgtgagttttgtcacagATACGGTGCAATCGGGGGGCCCTGACTGTCTTCCACCACCGTCAATA
CTCCACAACCTCACGATGCGGATTTCGGTCGTGATTGGGTGGGACCTGGGGGCTACGTTGCATCGAATAAAGCCGCC
CAACTTGGCTTAAAAgtgtgtataaaaatgcgtttttttgcccctataataaccagtttttagaCAGTATGTATAGA
GAAAGAACC

>dld/KI (P45S)
gtcactcgataatgtgagttttgtcacagATACGGTGCAATCGGGGGGCCCTGACTGTCTTCCACCACCGTCAATA
CTCCACAACCTCACGATGCGGATTTCAGTGGTCATCGGGTAAATGATCTGGGGGCTACGTTGCATCGAATAAAGCCGCC
CAACTTGGCTTAAAAgtgtgtataaaaatgcgtttttttgcccctataataaccagtttttagaCAGTATGTATAGA
GAAAGAACC
```

***Cyt-b5-fad* gene**

```
>Cyt-b5-fad/Vermillion (G349/N358)
ATCTTCCACGACGGTGACGCCCCACGgcaagtaccgagagacccatttcgacccatgacacccagtttttagGTCA
GACACCGACTACGACTGGGGCTTGGGTCGAAGTGGACGCTATCATGGACCGGAATGAAATCACAGGATCCATTTC
TGGTCCTTACGAACCTTGGGGACCATGCATTACACCACATGTTCCCAACTCTGGACCATGGGACTTTGGAGCTTTT
GTACCCAACCTTTCAGGA

>Cyt-b5-fad/KI (G349S/N358H)
ATCTTCCACGACGGTGACGCCCCACGgcaagtaccgagagacccatttcgacccatgacacccagtttttagGTCA
GACACCGACTACGACTGGGGCTTGGGTCAGCTTGATGCAATAATGGACCGGATGAAATCACAGGATCCATTTC
TGGTCCTTACGAACCTTGGGGACCATGCATTACACCACATGTTCCCAACTCTGGACCATGGGACTTTGGAGCTTTT
GTACCCAACCTTTCAGGA
```

Figure

14: Sequences of *dld* and *Cyt-b5-fad* targeted regions before and after the knock in. Yellow colored letters indicate the synonymous nucleotide changes between the original sequences from the *vermillion*^{white} strain and the modified ones, whereas red colored letter indicate non-synonymous changes. Marked-text in the sequences indicate: PAM (Red), P45S (*dld*) /G349S (*Cyt-b5-fad*) substitutions (yellow), N358H (*Cyt-b5-fad*) substitution (light green), sgRNA recognition sites (magenta) and RFLP sites (dark green).

At the onset of these experiments, it was important to test and optimize, if needed, the existing protocol for embryo microinjection. For this purpose, preliminary microinjections were performed in order to measure the survival rate of the injected embryos compared to non-injected ones. In *T.castaneum*, the default protocol for this technique involves the microinjection of embryos in dry air. However, with these conditions, when the injected mix was viscous (as is normally the case in CRISPR

experiments with Cas9 protein), this resulted in the very frequent clogging of the needle. The use of different needles with shorter or longer tapers didn't solve the clogging problem. In order to overcome this problem, I attempted microinjections in embryos immersed in halocarbon oil (as done in *Drosophila*). Although previous studies had indicated that the use of halocarbon oil in microinjections of *T.castaneum* resulted in a considerable reduction in the survival rate, the embryogenesis itself seemed to be unaffected (Benton et al., 2013). A possible cause for the observed mortality is that hatched larvae are unable to escape from the oil and end up drowning. In order to test that hypothesis, both injected and non-injected embryos were removed from halocarbon oil around one day before their expected hatching and placed on a Whatman paper to absorb any residual oil. Including this step, the measured survival rate in halocarbon oil was very similar to embryos processed in dry air (Table 1).

	Without dechoriation	With dechoriation in air	With dechoriation in halocarbon oil	With dechoriation and microinjection in air	With dechoriation and microinjection in halocarbon oil
Number of embryos at the beginning	100	100	100	100	100
Number of embryos hatched	73	56	55	32	38
Survival rate (%)	73	56	55	32	38

Table 1: Survival rate of non-injected and injected (with ddH₂O) *T.castaneum* embryos incubated at 32°C with or without immersion in halocarbon oil. Survival of non-dechorionated embryos was also measured in order to see the basic embryonic survival of the used *vermillion*^{white} strain.

The next step was to test the cutting efficiency of the Cas9 protein and the designed sgRNAs on the targeted *dld* and *Cyt-b5-fad* sequences. For this purpose, two different experiments were performed. The first one involved the in vitro digestion of PCR amplicons from the targeted loci (415bp for *dld* and 452bp for *Cyt-b5-fad*) after their incubation with Cas9 protein and their respective sgRNA. Gel electrophoresis of the treated samples showed a complete digestion (252bp /163 bp fragments in the case of *dld* and 288bp/164 bp fragments in the case of *Cyt-b5-fad*) (Figure 15).

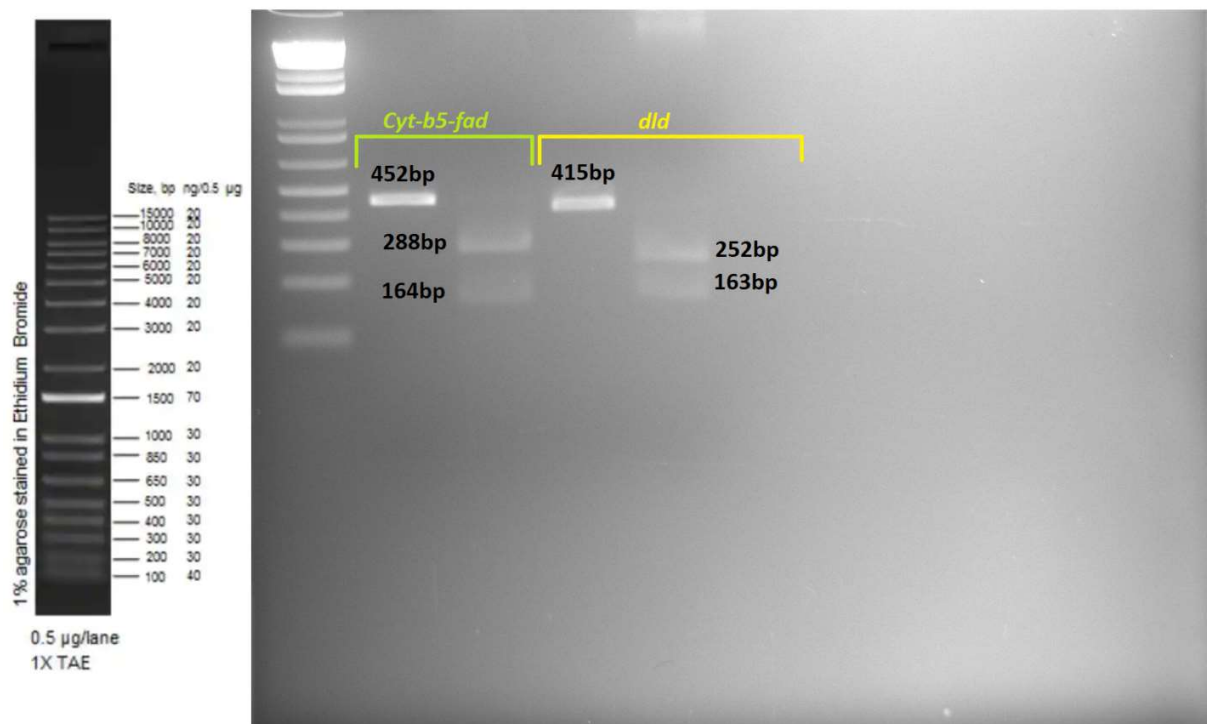


Figure 15: In vitro Cas9 cleavage assay for the *dld* and *Cyt-b5-fad* loci. The pattern of the used DNA ladder (1Kb+, Invitrogen) is shown on the left for reference.

The second assay involved a mismatch nuclease assay on a pool of animals injected with Cas9/sgrRNA complexes. That assay examines the activity of the Cas9/sgrRNA complexes on the genomic targets in vivo, by screening for nucleotide changes generated by the NHEJ repair mechanism of induced DSBs (Figure 16A). In more detail, this assay involves for each gene the denaturation and reannealing of PCR amplicons amplified from genomic DNA isolated from injected and non-injected animals (Figure 16A). Afterwards, these DNA samples are incubated with specific nucleases (such as CELI and T7 endonuclease I) that cut the dsDNA where mismatches are present (Figure 16A) and the separation of undigested homoduplexes from digested heteroduplexes by gel electrophoresis. Heteroduplexes are the result of Cas9/sgrRNA cleavage and NHEJ repair, providing a quantitative assay to assess the activity of sgRNAs in vivo (Figure 16B). This analysis demonstrated that a large fraction of the targeted *dld* and *Cyt-b5-fad* loci are cleaved with the designed sgRNAs in vivo.

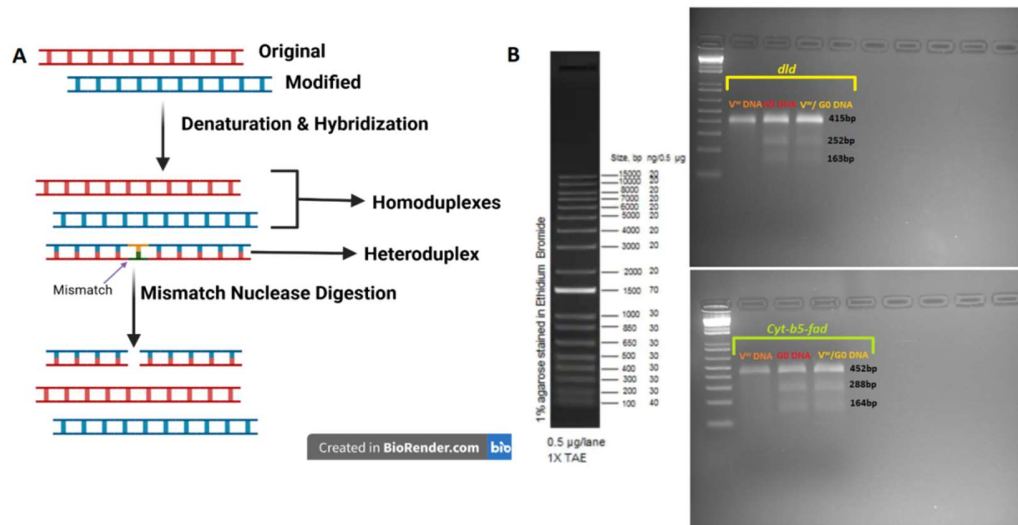


Figure 16: (A) Schematic representation of the mismatch nuclease assay created in BioRender.com. (B) Mismatch nuclease assay for the *dld*(top) and *Cyt-b5-fad*(bottom) loci. The acronyms indicate: V^W DNA= PCR fragment amplified from *vermillion*^{white} genomic samples, G0 DNA= PCR fragment amplified from G0 animal genomic samples, V^W/G0 = a 50:50 mix of the two. G0 DNA gives a digested pattern, because G0 animals are mosaic for the mutation, so both modified and unmodified DNA is present. The pattern of the used DNA ladder (1Kb+, Invitrogen) is shown on the left for reference.

Based on the encouraging results of the in vitro and in vivo assays, I proceeded with the CRISPR knock in experiments as planned, always keeping in mind that the efficiency of the CRISPR knock in experiments is much lower than the efficiency of CRISPR knock out experiments. Each ssODNs was added in the injection mixes together with the Cas9 protein and the corresponding sgRNA to generate the double sensitive line (targeting *Cyt-b5-fad*) and the double resistant line (targeting *dld*) (Figure 13). The results of these experiments are summarized in Table 2 shown below:

	<i>Cyt-b5-fad</i>	<i>dld</i>
Number of embryos injected	708*	738**
Number of G0 larvae hatched	22*	25**
Number of fertile G0 larvae reached adulthood	12*->9♀ and 3♂	15**->8♀ and 7♂
Embryo survival rate (%)	3.1	3.6
Larvae survival rate (%)	54.5	60

Table 2: Overview of the microinjection experiments for the creation of *dld* and *Cyt-b5-fad* knock in lines. (*)= Data from 5 independent experiments, (**) = Data from 6 independent experiments.

The survival rate of injected embryos to hatching was extremely lower than that observed in the pilot experiments (around 3% vs. 38%). In order to verify that this unexpected result was not related to toxic effects of halocarbon oil not observed in the previous experiments or possible contamination of the equipment, two rounds of microinjections with water only were performed. The survival rate of those was shown to the same levels with that of the first experiments (data not shown), indicating that there was not any particular problem with the injection protocol itself. A possible explanation is that due to the important role these genes have in mitochondrial metabolism, the disruption of their function in any tissue of the animal could lead to lethal phenotypes. This is further supported by the mortality of the hatched G0 larvae that failed to reach adulthood estimated at 40-45% (instead of 10-20% observed in the *vermillion*^{white}). In addition, any off-target activity that cannot be controlled in these experiments could also account for the observed lethality.

Despite this small number of survivors, I proceeded with their back-crossing to *vermillion*^{white} in order to screen for potential knock in events in the following G1 generation. More specifically, injected G0s were sexed at the pupal stage, were staged for a week to reach adulthood and sexual maturation, and were then back-crossed to *vermillion*^{white} beetles of the opposite sex for several weeks with weekly collections of their offspring. From each cross, the first batch of grown G1 larvae was used for genomic DNA (gDNA) extraction. The isolated gDNA from each of these pools of G1 animals was screened for possible knock in events using two different screening assays. The first one screened for the presence of the introduced RFLP sites present in the ssODNs by restriction digest of PCR amplicons amplified from the targeted loci (Figure 17A). Unfortunately, gel electrophoresis did not show the characteristic size pattern expected for knock in events in the 15 *dld*-targeted lines and the 12 *Cyt-b5-fad*-targeted lines (279bp/136bp for the *Clal* digest of *dld* locus and 256bp/156bp for the *Bam*HI digest of *Cyt-b5-fad* locus) (Figure 17A). The second assay used specific primers for each of the modified genes to selectively identify by PCR any knock in events. Confirming the results of the first assay, gel electrophoresis did not show the expected sizes (187bp for *dld* locus and 182bp for *Cyt-b5-fad*) for any of the lines (Figure 17B).

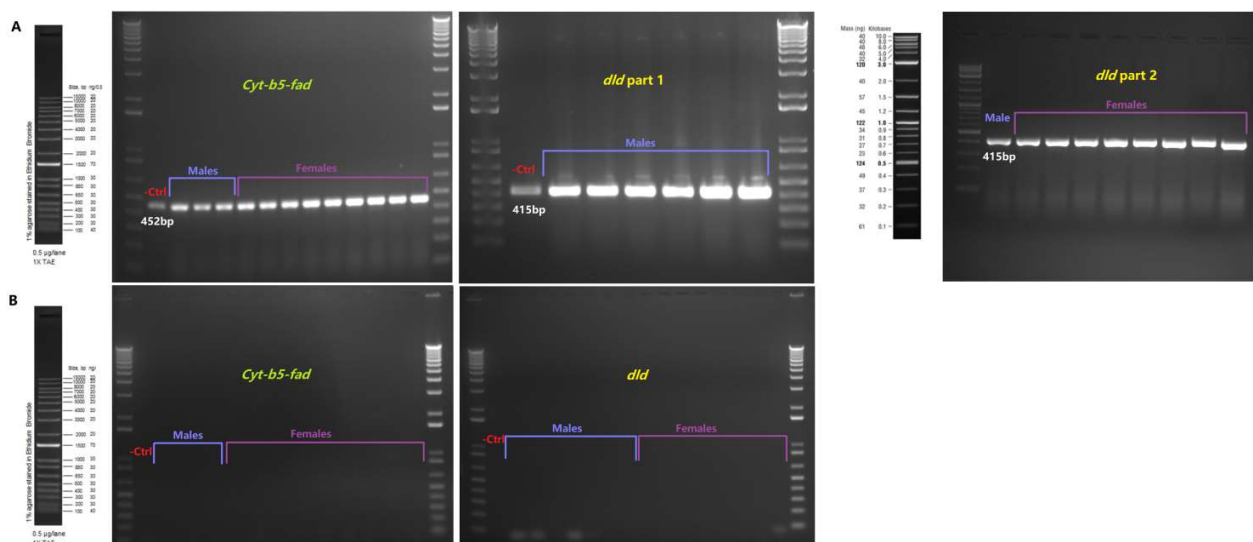


Figure 17: (A) RFLP and (B) PCR screening of G1 animal pools for both loci. As a negative control (-Ctrl), genomicDNA from the *vermillion*^{white} strain was used. The patterns of the used DNA ladders are shown on the left for reference.

As a last experiment for this part of my thesis, I checked for the presence of modified *dld* or *Cyt-b5-fad* alleles in these G1 pools using the same mismatch nuclease assay employed in the original in vivo testing of the Cas9/sgRNA complexes in injected embryos. That first experiment had indicated a relatively high number of modified alleles in G0s, while this new analysis aimed to assess the presence of modified alleles in the gametes that gave rise to the assayed pools of G1s. Among the 27 lines assayed, only one G1 pool from the *Cyt-b5-fad*-targeted beetles had a pattern that suggested the presence of one or few G1s with modified *Cyt-b5-fad* alleles among the progeny from this one G0.

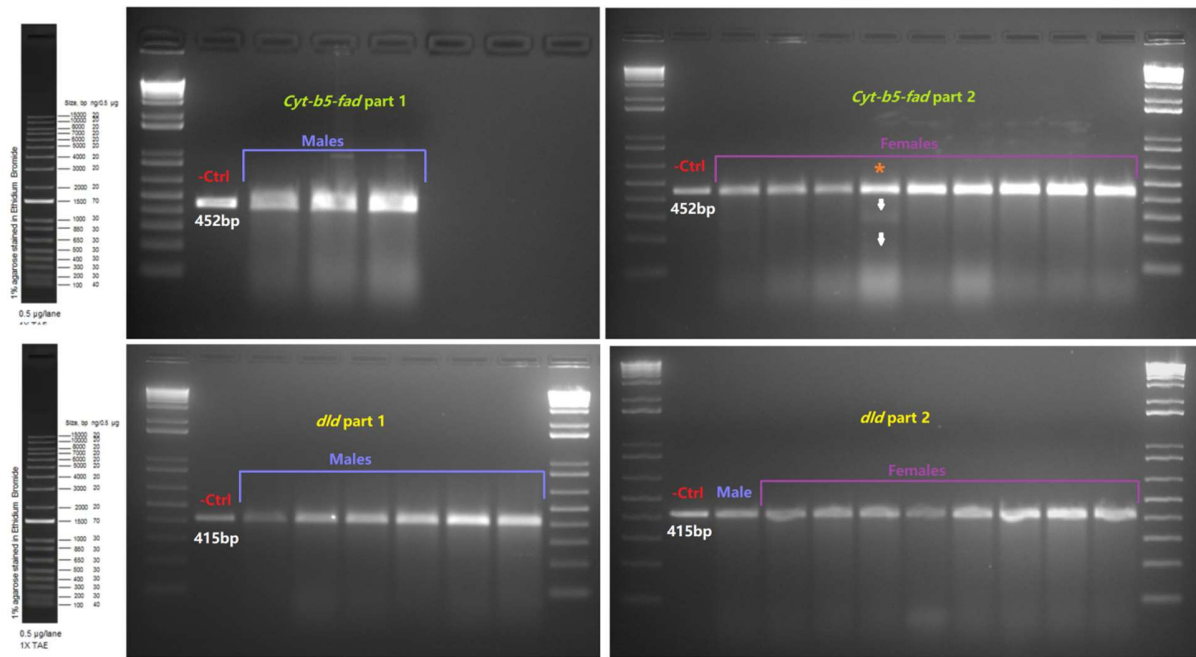


Figure 18: Mismatch nuclease assay screening of G1 animal pools for both loci. As a negative control (–Ctrl), genomic DNA from the *vermillion*^{white} strain was used. The asterisk indicates the only pool of G1 beetles exhibiting the expected pattern (288bp+164bp fragments shown by the white arrows) for *Cyt-b5-fad* knock out. The pattern of the used DNA ladder (1Kb+, Invitrogen) is shown on the left for reference.

These results indicate that 8.3% (1/12) of the *Cyt-b5-fad*-injected G0s and 0% (0/15) of the *dld*-injected G0s transmit modified alleles to their G1 progeny. Therefore, a much larger number of lines need to be generated and analyzed for knock in events in the future considering the low frequency of CRISPR/Cas9-based knock in compared to simple knock out (i.e. allele modification) approaches. It remains to be seen whether these low rates of gene editing are associated with the efficiency of these particular sgRNAs, the efficiency of the ssODN approach in *T. castaneum*, the mortality caused by disrupting any of these two genes, or a combination of these factors.

*4. NHEJ-based CRISPR knock in for in vivo testing of the UAS/Gal4 binary gene expression system in *Parhyale hawaiiensis**

4.1 Introduction

Binary expression systems: A valuable tool for functional genetic analysis

Besides the genome editing tools that were described earlier, there are other tools used for the identification of a gene's functional role. One of the most important tools are the binary gene expression systems. As the name implies, they consist of two fundamental components: the driver and the responder (Figure 19) (Viktorinová and Wimmer, 2007), (Riabinina and Potter, 2016). The driver contains a transactivator gene which is regulated by an endogenous *cis*-regulatory element (enhancer+promoter) of the studied organism. The responder (a.k.a. effector) contains a regulatory region, which can be bound by the transactivator protein, coupled to a core promoter that can drive expression of a gene of interest (Figure 19) (Viktorinová and Wimmer, 2007)(Riabinina and Potter, 2016). These two parts are typically uncoupled in two different laboratory strains of the studied organism and the responder is silent (Figure 19) (Viktorinová and Wimmer, 2007)(Riabinina and Potter, 2016). After crossing these two strains, in progeny of these crosses the transactivator protein will interact with its DNA binding region in the responder cassette and will activate the expression of the downstream gene in the cells where the endogenous regulatory element is active (Figure 19)(Viktorinová and Wimmer, 2007)(Riabinina and Potter, 2016). This way, the spatiotemporal expression pattern of a gene of interest can be easily controlled allowing for targeted expression in any desired tissue and developmental stage (Viktorinová and Wimmer, 2007)(Riabinina and Potter, 2016). As a result, by changing the expression pattern of a selected gene, the binary expression system can be any extremely useful in the analysis of a gene's function.

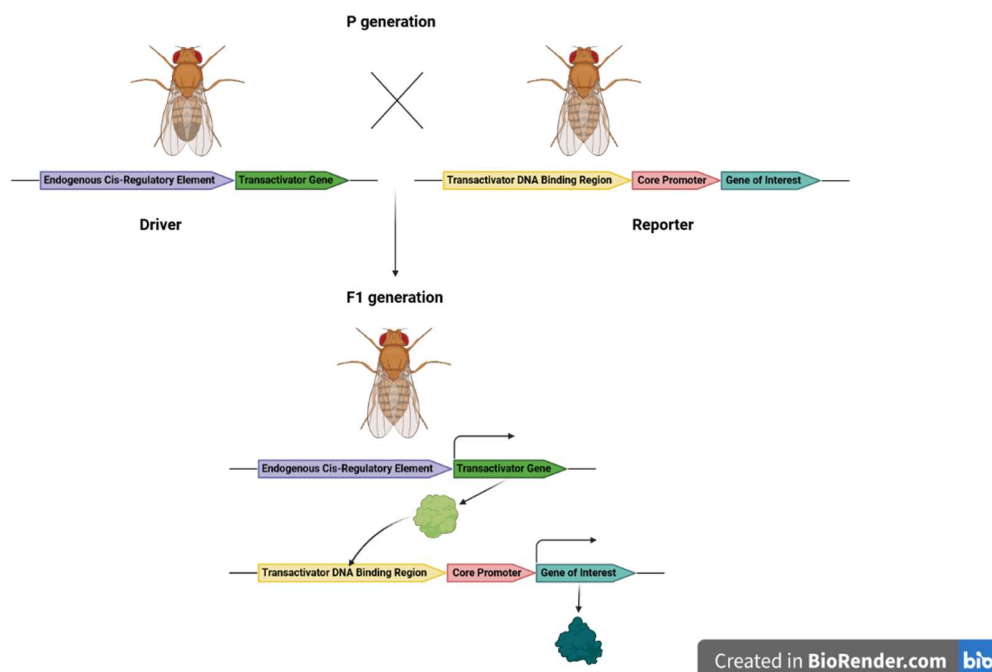
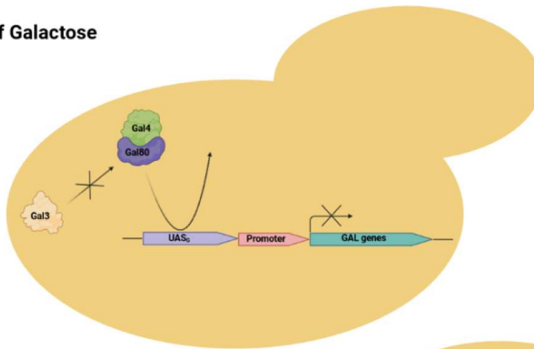


Figure 19: Overview of binary gene expression systems in *Drosophila*. Created in BioRender.com.

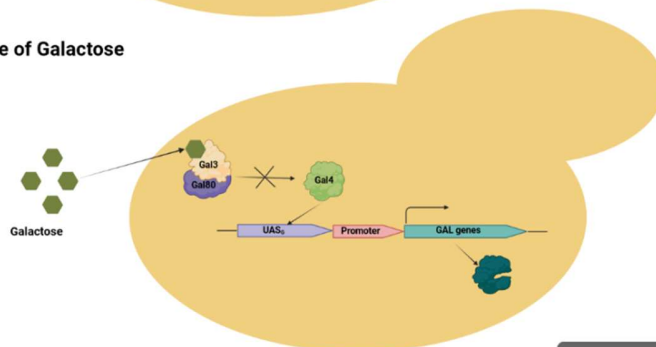
The binary expression system UAS/Gal4

The most widely used binary expression system is UAS/Gal4, which uses components from a regulatory network from the budding yeast *Saccharomyces cerevisiae* that controls the expression of genes encoding enzymes participating in galactose metabolism (Watson, 2014) (Traven et al., 2006). More precisely, the fundamental parts of this network are a transcriptional activator called Gal4 and its responsive regulatory sequence called UAS_G (galactose responsive Upstream Activating Sequence) (Figure 20) (Watson, 2014) (Traven et al., 2006). In the absence of galactose, Gal4 forms a complex with a transcriptional repressor called Gal80, which prevents it from binding to the UAS_G and activate the expression of downstream target genes (Figure 20A) (Watson, 2014) (Traven et al., 2006). However, when galactose is accumulated in the cell, it acts as an allosteric ligand for another protein called Gal3 and changes its conformation (Watson, 2014) (Traven et al., 2006). In this form, Gal3 can interact with Gal80 and prevent it from binding to Gal4, thus allowing Gal4 binding to UAS_G and expression of UAS_G controlled genes (Figure 20B) (Watson, 2014) (Traven et al., 2006).

A) Absence of Galactose



B) Presence of Galactose



Created in BioRender.com 

Figure 20: Overview of the gene regulatory pathway for galactose metabolism in *Saccharomyces cerevisiae*. Created in BioRender.com.

This regulatory network has been studied in great depth in *S. cerevisiae* during the previous decades in order to understand the mechanisms behind gene expression, something that later allowed the use of its two fundamental components (Gal4 and UAS_G) for the creation of the first binary expression system in 1988 by two different research teams (Kakidani and Ptashne, 1988) (Webster et al., 1988). The researchers in these teams tested the function of UAS/Gal4 system in two different mammalian cell lines (CHO and HeLa) (Kakidani and Ptashne, 1988) (Webster et al., 1988). The first in vivo use in a multicellular organism came five years later with the successful establishment of the system in

Drosophila melanogaster (Brand and Perrimon, 1993), making it one of the most valuable molecular tools used in this model species up until today (Duffy, 2002) (Elliott and Brand, 2008). In later years, there were several attempts to establish UAS/Gal4 in other animal species, including both invertebrates such as the malarian mosquito *Anopheles gambiae* (Lycett et al., 2012) and the flour beetle *Tribolium castaneum* (Schinko et al., 2010), as well as vertebrates such as the teleost fishes *Danio rerio* (Scheer and Campos-Ortega, 1999) and *Oryzias latipes* (Grabher and Wittbrodt, 2004).

This extensive study of UAS/Gal4 as a tool or as a model for gene regulation has led to the creation of a large number of different variants for both components. In the case of Gal4, the alterations have focused on the two fundamental domains of the protein: the DNA binding domain (which interacts with the UAS_G) and the transactivation domain (which recruits the transcriptional machinery needed for the gene expression) (Watson, 2014) (Ma and Ptashne, 1987). These domains are located on the N-terminal and the C-terminal regions of the protein, respectively (Watson, 2014) (Ma and Ptashne, 1987). The rest of the protein doesn't seem to have any functional role necessary for gene expression. This observation led to the development of the first Gal4 variant, which lacked the intermediate part of the sequence fusing together the DNA binding and transactivation domains (Ma and Ptashne, 1987). This altered form of Gal4 is known as Gal4Δ (Figure 21A) and proved to be more efficient in activating gene expression than the wild type form (Horn et al., 2003) (Viktorinová and Wimmer, 2007).

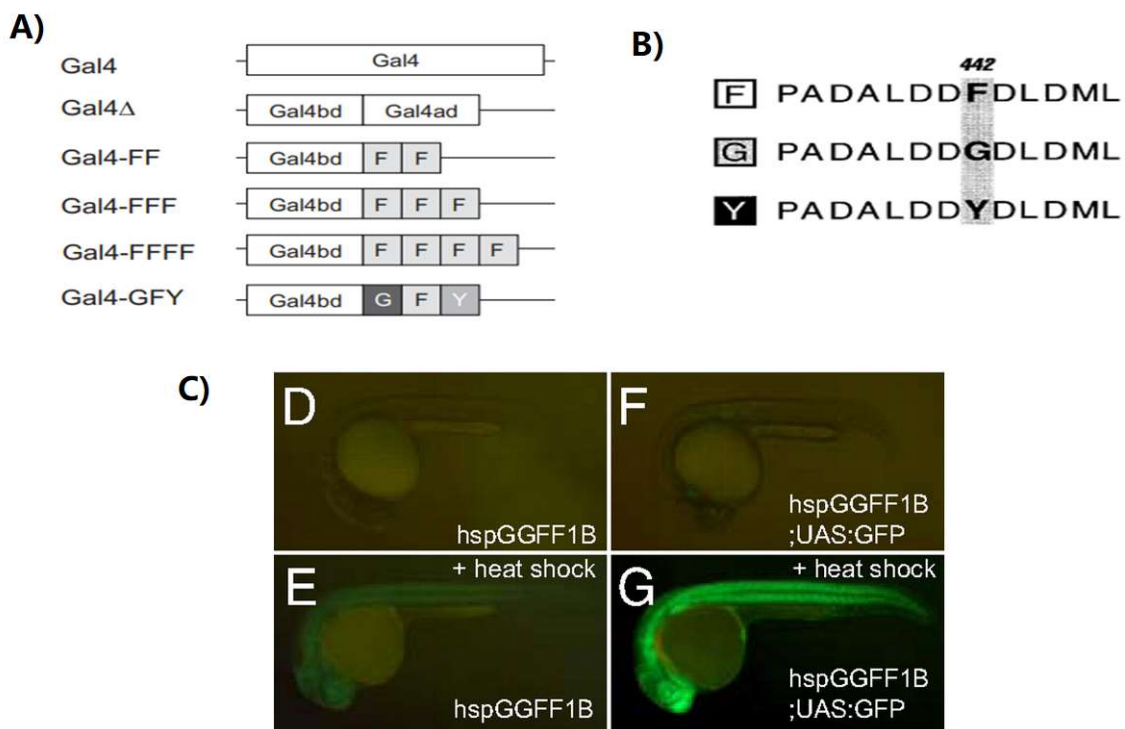


Figure 21: (A) Schematic representation of several Gal4 variants. (B) Amino acid sequences of G/F/Y domains. Their distinguishing position is marked. (C) *Danio rerio* UAS/Gal4 transgenic lines expressing the GGFF transactivator under the regulation of a heat shock promoter. Individuals before and after heat shock are shown. (A) was taken and modified from Lynd and Lycett, 2011, (B) from Baron et al., 1997 and (C) from Asakawa et al., 2008.

Another important Gal4 variant is Gal4-VP16, in which the transactivation domain from the VP16 transcriptional factor of HSV-1 (Herpes Simplex Virus 1) was fused to the DNA-binding domain of Gal4 (Sadowski et al., 1988). This chimeric protein proved to be an extremely potent transcriptional activator responsible for transcriptional squelching (a phenomenon in which a transcriptional activator inhibits the expression of other genes due to its very strong binding and sequestration of general transcriptional factors) (Sadowski et al., 1988) (Gill and Ptashne, 1988). For that reason, a group of researchers tried to create alternative forms of the VP16 transactivation domain that could retain the efficiency of the original domain but without any undesired effects (Baron et al., 1997). The group focused on very small regions of the VP16 transactivation domain, which are rich in acidic residues and only 12 amino acids in length, and designed three synthetic variants named F, G and Y differing in their eighth position (Figure 21A and B) (Baron et al., 1997). These three different peptides were later fused in different combinations, generating very efficient transactivation domains (Figure 21A) (Baron et al., 1997) (Lynd and Lycett, 2011). Some of them activated transcription as strongly as the original VP16 (like the 3xF domain) (Baron et al., 1997) (Lynd and Lycett, 2011), while others were even more powerful (such as the 4xF domain) (Baron et al., 1997), (Lynd and Lycett, 2011). However, regardless of their efficiency, all combinations exhibited vastly reduced toxicity in comparison to VP16 (Baron et al., 1997).

In other Gal4 variants, a specific part of the transcription factor was fused to a fluorescent protein (Asakawa et al., 2008). This allows the visualization of the protein in the embryos where it is expressed, which is convenient for monitoring the driver component in the desired conditions (Asakawa et al., 2008). An example of such variants is eGFP-Gal4FF (GGFF for short), which is one of the best optimized versions of Gal4 in terms of efficiency and toxicity for use in *Danio rerio* (Figure 21C) (Asakawa et al., 2008).

Finally, regarding the creation of UAS_G variants, the alterations were focused on the number of Gal4 binding sites presented in each sequence. The wild-type UAS_G is formed by the repetition of four Gal4 binding sites (also known as UAS sites) (Watson, 2014). However, during experimentation, variants with a greater number of UAS sites have been tested, with the two best known being 5xUAS and 14xUAS (Brand and Perrimon, 1993) (Rørth, 1996). The efficiency of those sequences as regulatory elements is shown to depend on the type of Gal4 variant combined with them and the studied model organism. For example in *Anopheles gambiae*, Gal4Δ was much more effective in activating gene expression when used with regulatory sequences with more UAS sites, whereas Gal4FFFF had a standard efficiency that was independent of the regulatory sequence with which it was paired (Lynd and Lycett, 2011). Another interesting observation comes from research trying to establish UAS/Gal4 in *Danio rerio*, where regulatory sequences with a large number of UAS sites were much more ineffective compared to smaller ones (Akitake et al., 2011). The reason for this paradox is that UAS sites are rich in GC content, making them vulnerable to epigenetic silencing by methylation (Akitake et al., 2011). This problem was not previously observed because Gal4/UAS has been mainly applied in *Drosophila melanogaster* that has extremely low levels of DNA methylation (Deshmukh et al., 2018).

Distal-less: A key gene in the development of arthropod appendages

One of the distinguishing characters of the arthropod phylum is the presence of jointed appendages in all species. Understanding the developmental mechanisms that control appendage formation in different arthropod lineages, including the conservation and divergence of these mechanisms over the course of evolution, is an important field of research in the field of Evolutionary Developmental Biology.

So far, most of our knowledge on appendage development in arthropods comes mainly from insects, in particular *Drosophila melanogaster*. Arthropod appendage patterning along their proximal-distal axis requires four highly conserved genes, known as leg gap genes: *extradenticle*(*exd*), *homothorax*(*hth*), *dachshund*(*dac*) and *Distal-less*(*Dll*)(Dong et al., 2001)(Estella et al., 2012).

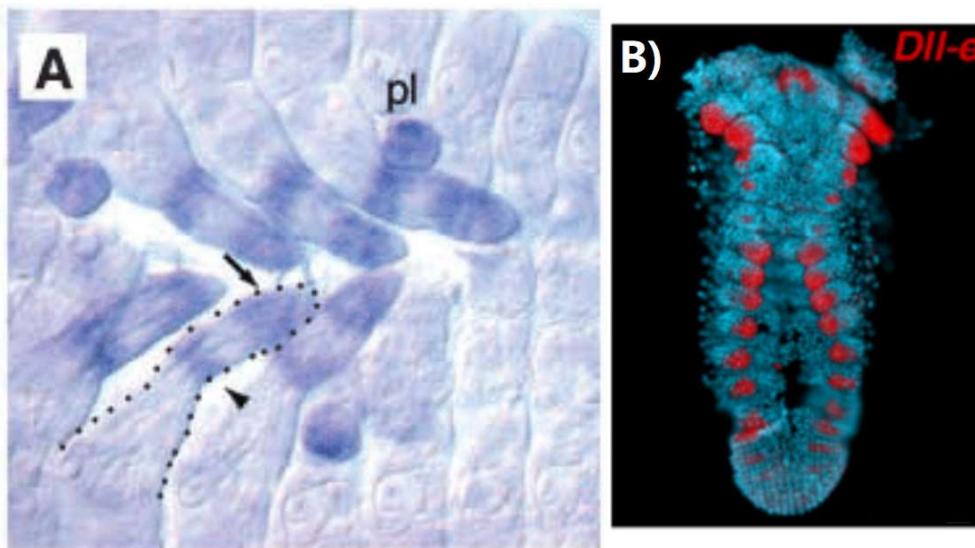


Figure 22: Expression

of the *Distal-less* (*Dll*) gene in the limbs of *Tribolium castaneum* (A) and *Parhyale hawaiiensis* (B) embryos. In part (A) an individual limb is outlined by a dotted line and *Dll* expression in the more proximal “ring” region is shown by the arrowhead and the in the more distal “sock” region by the arrow. This ring-and-sock expression pattern of *Dll* is characteristic to all neopterygote insects (Schaeper et al., 2013). *Dll* is also transiently expressed in the abdominal pleuropodium (pl). (A) was taken from Beermann et al., 2004, whereas (B) from Liubicich et al., 2009.

Among these genes, *Dll* is the earliest known marker expressed in the nascent limb primordia (Estella et al., 2012). Early and later phases of *Dll* expression are controlled by the *decapentaplegic* (*dpp*) and *wingless* (*wg*) signaling pathways (Estella et al., 2012). In *Drosophila*, *Dll* is first expressed throughout the limb primordia, but its expression is later localized in the distal parts of the limbs (telopodite) (Estella et al., 2012). *Dll* mutants display truncated limbs where their distal parts are missing (hence the name *Distal-less*) (Estella et al., 2012).

***Parhyale hawaiiensis*: An emerging crustacean model species in evolutionary and developmental biology**

Parhyale hawaiiensis is an amphipod crustacean that was first introduced as a model species for biological research in the laboratory of Nipam Patel in 1997 (Rehm et al., 2009). It is one of the best studied crustacean species, as it has several characteristics that allowed it to become a very promising

arthropod model in the laboratory(Browne et al., 2005), (Rehm et al., 2009)(Stamataki and Pavlopoulos, 2016).

In terms of ecology, *P.hawaiensis* is a small detritivore with a worldwide distribution, inhabiting the shallow waters of the intertidal zone in all tropical and subtropical seas(Browne et al., 2005)(Rehm et al., 2009). It is commonly found in mangrove swamps, where large population can be sustained due to the accumulation of decaying plant material (Browne et al., 2005)(Rehm et al., 2009). Shallow-water habitats like these are naturally subject to rapid changes in temperature and salinity (Browne et al., 2005)(Rehm et al., 2009). As a result, *P.hawaiensis* can tolerate different kinds of environmental changes and can thrive in large colonies under standardized laboratory conditions(Browne et al., 2005)(Rehm et al., 2009).

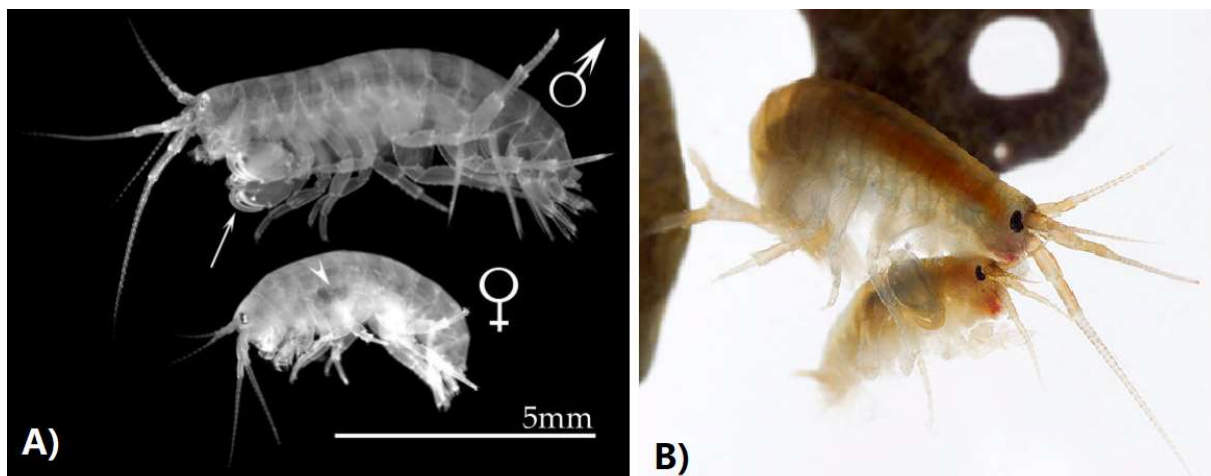


Figure 23: (A) Male and Female Individuals of *Parhyalehawaiensis*. The arrows indicate the enlarged second pair of gnathopods in the male and the egg brood pouch in the female. (B) A mating pair of *Parhyalehawaiensis*. (A) was taken from Browne et al., 2005, whereas (B) from Paris et al., 2022.

The life cycle of the species is relatively short, lasting around 2 months at 26°C (Figure 24)(Browne et al., 2005)(Rehm et al., 2009). *P.hawaiensis* is sexually dimorphic with adult males being bigger in size and exhibiting an enlarged second pair of gnathopods used for holding females during copulation (Figure 23B)(Browne et al., 2005)(Rehm et al., 2009)(Stamataki and Pavlopoulos, 2016). After that, the females are released and deposit 5-30 fertilized eggs into a ventral brood pouch (Figure 23A)(Browne et al., 2005)(Rehm et al., 2009)(Stamataki and Pavlopoulos, 2016). This pouch is characteristic of all crustaceans in the superorder Peracarida(Poore, 2005) and is formed after mating by special plate-like structures(oostegites) at the basis of the first four pairs of thoracic legs (Browne et al., 2005)(Rehm et al., 2009). The eggs remain in the pouch during embryogenesis is complete that lasts 10 days at 26°C (Figure 24)(Browne et al., 2005)(Rehm et al., 2009)(Stamataki and Pavlopoulos, 2016). Embryonic development has been divided into 30 discrete stages based on phenotypic and molecular markers (Browne et al., 2005)(Rehm et al., 2009). Embryos of each stage can be easily collected from gravid females anesthetized with CO₂ gas without harming or killing them. Dissected embryos can be kept in petri dishes with artificial sea water(Browne et al., 2005), (Kontarakis and Pavlopoulos, 2014)(Stamataki

and Pavlopoulos, 2016). The year-round breeding habits of the species and the easiness of maintaining very large population in the lab give access to hundreds of embryos on a daily basis for experimentation (Browne et al., 2005) (Rehm et al., 2009) (Stamatakis and Pavlopoulos, 2016).

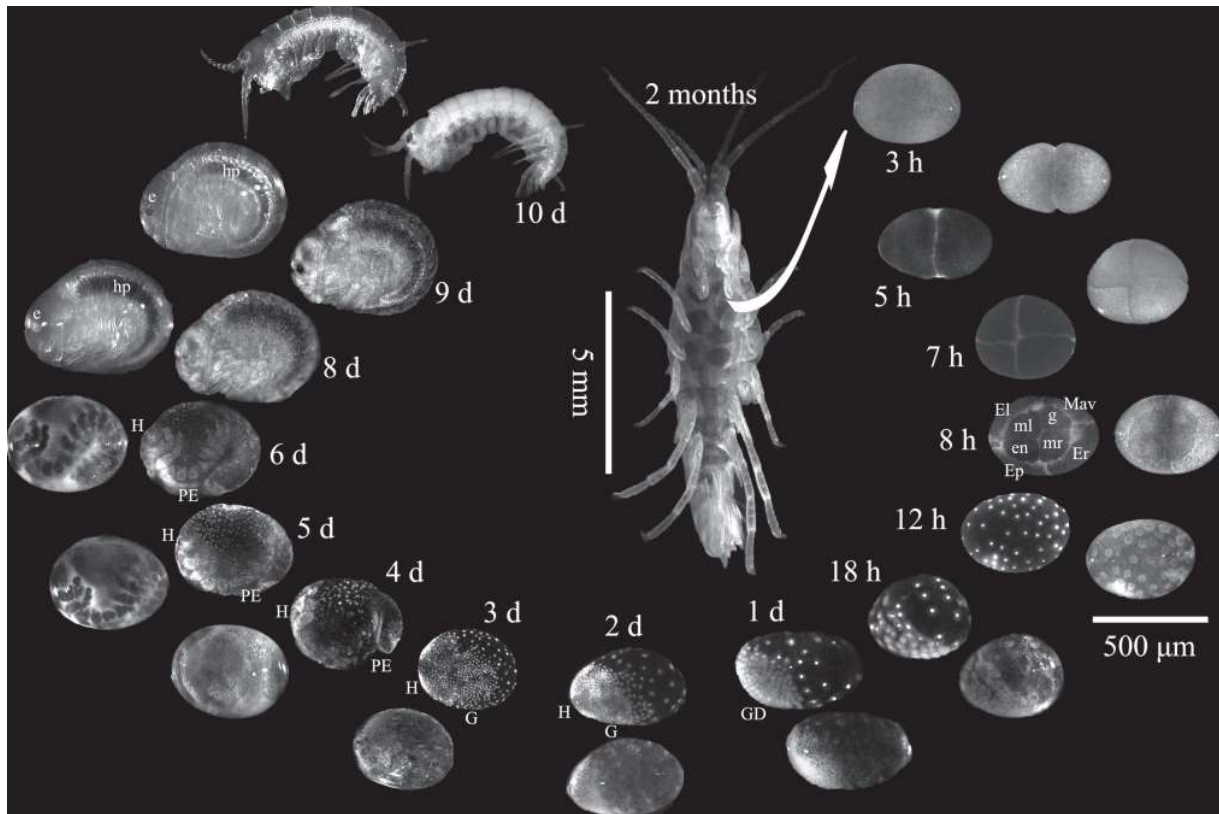


Figure 24: Life cycle of *Parhyale hawaiiensis*. Acronyms in the 8h (8-cell) stage indicate the fates of the individual blastomeres: El = Left Anterior Ectoderm, Er = Right Anterior Ectoderm, Ep = Posterior Ectoderm, Mav = Anterior Somatic Mesoderm and Visceral Mesoderm, ml = Left Posterior Somatic Mesoderm, mr = Right Posterior Somatic Mesoderm, en Endoderm, g = Germline. Image taken from chapter 16 in Boutet and Schierwater, 2022.

Some other embryonic characteristics that make *P. hawaiiensis* an attractive model species is that its eggs are relatively large in size (around 500 µm) and can be collected after fertilization at the 1-cell stage. These features, together with the fact that the embryos follow a holoblastic (total) cleavage mode (compared to the superficial one in the majority of hexapods), enable a variety of different embryological manipulations such as microinjection and cell ablations (Browne et al., 2005) (Rehm et al., 2009) (Stamatakis and Pavlopoulos, 2016). The embryos are also optically clear and suitable for live imaging and detailed microscopic analysis with fluorescent markers (Browne et al., 2005) (Rehm et al., 2009). With the exception of secondary sex characters, *P. hawaiiensis* hatchlings are morphologically similar to the adults (direct developers), presenting a complete set of all segments and associated appendages (Browne et al., 2005) (Rehm et al., 2009). Unlike in holometabolous insect models such as *Drosophila melanogaster* and *Tribolium castaneum*, it is possible to study the development of most adult body structures during embryogenesis (Browne et al., 2005) (Rehm et al., 2009).

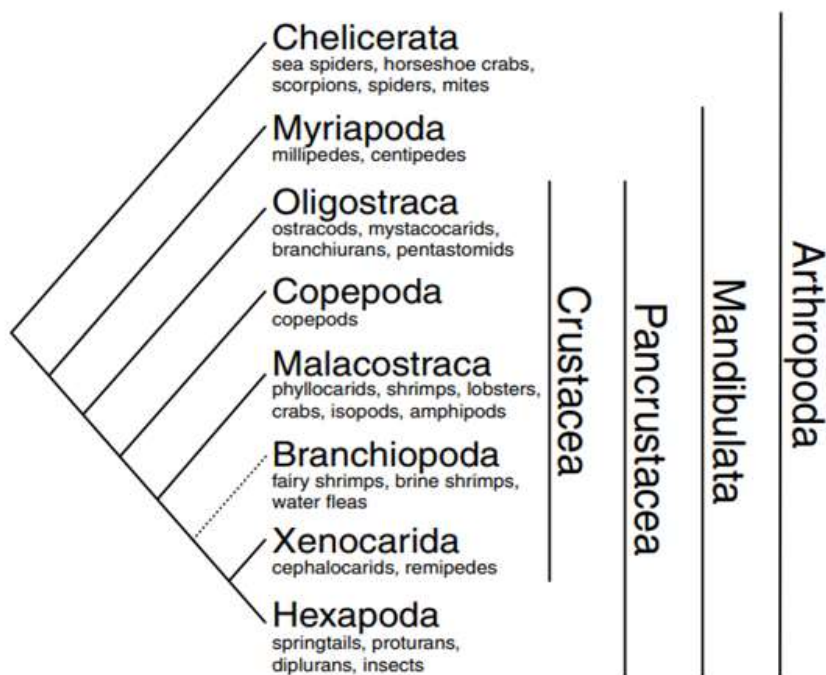


Figure 25: Phylogenetic tree of different arthropod sublineages. Image taken from Stamatakis and Pavlopoulos, 2016.

Finally, one last important characteristic of *P.hawaiensis* is its phylogenetic position (Figure 25). The majority of arthropod model species used in biological research are insects, which are essentially terrestrial crustaceans (Browne et al., 2005) (Rehm et al., 2009) (Stamatakis and Pavlopoulos, 2016). More precisely, the most recent phylogenetic studies show that the hexapod lineage evolved from within the crustaceans forming with them a monophyletic taxon, the Pancrustacea (Figure 25) (Browne et al., 2005) (Rehm et al., 2009) (Stamatakis and Pavlopoulos, 2016). Therefore, the establishment of crustacean model species is essential for the understanding of the evolution and diversification of hexapods and arthropods in general. A number of crustacean species have been introduced as experimental models, such as the cladoceran *Daphnia pulex* (Colbourne et al., 2011) and the anostracan *Artemia franciscana* (Averof and Akam, 1995) (Copf et al., 2004). However, they are not genetically tractable to the same extent like *P.hawaiensis* where a variety of molecular and developmental experimental protocols have been established with great success (Pavlopoulos and Averof, 2005) (Liubicich et al., 2009) (Özhan-Kizil et al., 2009) (Kontarakis et al., 2011) (Nast and Extavour, 2014) (Kao et al., 2016). Finally, as an amphipod, *P.hawaiensis* is a member of Malacostraca (Figure 25), a class that includes the majority of commercially important crustaceans such as crabs, lobsters and prawns (Kao et al., 2016). Research on *P.hawaiensis* can be extremely useful for the improvement of methods used in the aquaculture of malacostracan food crop species (Kao et al., 2016).

4.2 Results and Discussion

The second part of my thesis involved the use of a different CRISPR knock in approach to test in vivo the UAS/Gal4 binary expression system in *P.hawaiensis*. Previous work done in the lab on this topic has indicated that Gal4 and Gal4GFY were the most efficient transactivators among variants assayed (Gal4, Gal4Δ, Gal4FFF and Gal4GFY) (Chalkia Georgia, 2021). The efficiency of the system was higher when these variants were tested with 14xUAS responder constructs compared to 5xUAS ones (Chalkia Georgia, 2021). However, all of these assays measured the activity of those binary system components from extrachromosomal plasmid templates and did not involve their insertion into the genome of *P.hawaiensis*.

My study involved the targeted integration of the UAS/Gal4 components in the animal's genome using a previous method developed in the lab for the HDR-independent CRISPR knock in of entire donor plasmids into the *Distal-less(Dll)* locus of *P.hawaiensis* (Figure 26A) (Kao et al., 2016). In more detail, a specific plasmid was used as a donor template which contained a copy of the *Dll* coding sequence coupled in frame with the T2A peptide sequence and a histone (PhH2B) tagged version of the red fluorescent protein Ruby2 (Figure 26A) (Kao et al., 2016). T2A belongs to a family of self-cleaving peptides (known as 2A peptides) found in several viral genomes and are useful for bicistronic constructs (Liu et al., 2017). The exact mechanism of 2A peptide action is not very well documented yet, however the predominant hypothesis is that they prevent the formation of a peptide bond between the two connected ORFs (*Dll* and the gene of interest in this case) by ribosomal skipping during the translation of the bicistronic mRNA (Liu et al., 2017) (Sharma et al., 2012) (Donnelly et al., 2001b). T2A is specifically isolated from the genome of 2A-TaV, a virus infecting the Limacodid moth *Thosea asigna* (Pringle et al., 1999) (Donnelly et al., 2001a) (Liu et al., 2017).

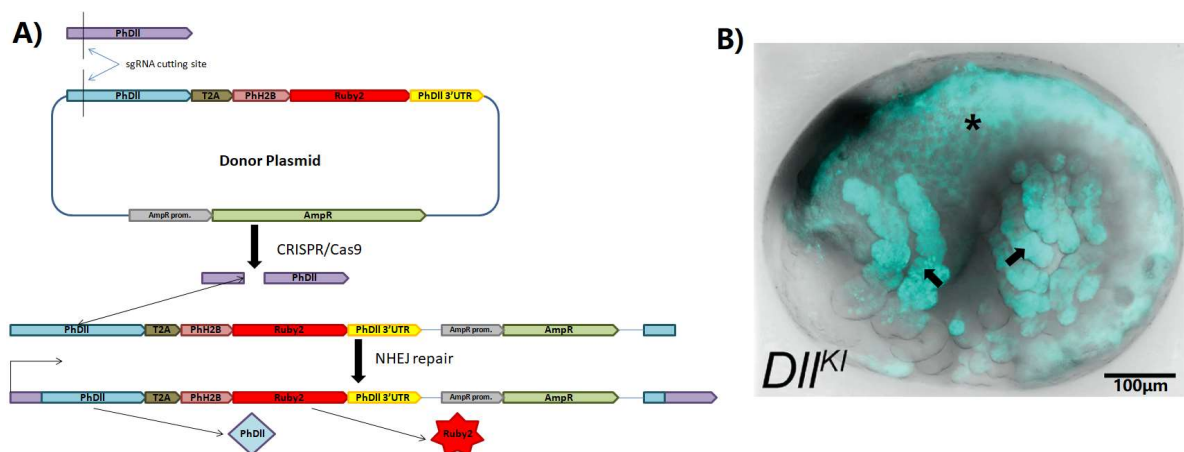


Figure 26: (A) Schematic representation of the CRISPR NHEJ knock in approach used by Kao et al. 2016. (B) *P.hawaiensis* *Dll* knock in embryo showing fluorescence in the distal regions of the limbs (arrows). Asterisk indicates autofluorescence of the gut. Scale bar is at 100μm. (B) is modified from Kao et al., 2016.

The protocol for CRISPR-based editing of the *Dll* locus in *P.hawaiensis* is very well optimized, making it a valuable platform to test in vivo the UAS/Gal4 combinations (Kao et al., 2016). This CRISPR knock in

approach uses a single sgRNA that efficiently cuts the *Dll* coding sequence at the same position in the *Dll* genomic locus and the donor plasmid, generating a condition where the linearized plasmid can be inserted by the NHEJ repair mechanism directly into the *Dll* locus (Figure 26A)(Kao et al., 2016). Integration of the linearized plasmid in the appropriate orientation and open reading frame restores the *Dll* ORF in a bicistronic mRNA that also encodes the nuclear fluorescent reporter (or the Gal4 variant) expressed in all cells where *Dll* is expressed(Figure 26A)(Kao et al., 2016). The screening for knock-in events is performed in injected G0 embryos based on fluorescent reporter expression in the *Dll* pattern, simplifying the identification of those rare knock-in events. In addition, measuring the number of G0 embryos with truncated limbs (that result from NHEJ-based *Dll* knock out) provides an easy phenotype to monitor the efficiency of Cas9/sgRNA-mediated DSBs at the targeted *Dll* locus. Finally, keeping in these experiments only the early 1-cell injected embryos increases the chances of recovering knock in events, because the Cas9/sgRNA complexes can target the genome early on and generate animals with low levels of mosaicism with most cells carrying the same genomic modification(s).

The new donor plasmids generated for this project had the coding sequence encoding the GGFF transactivator gene cloned in frame downstream of the *Dll*-T2A sequence. The same donor plasmid carried also in another position the responder cassette which was either 5xUAS-PhA5C-PhH2B-mCherry or 14xUAS-PhA5C-PhH2B-mCherry (Figure 27). The choice of PhA5C as the core promoter element coupled to either 5xUAS or 14xUAS sites was based on previous extrachromosomal activity assays carried out in the lab(Archontidis Themis, 2020)(Chalkia Georgia, 2021). PhA5C contains the 5'UTR and putative promoter sequences from the *Actin5C1* housekeeping gene of *P.hawaiensis*(Archontidis Themis, 2020). GGFF was selected over other Gal4 variants because it is green fluorescently labeled and simplifies the phenotypic screening of injected G0 embryos with successful in-frame knock in events. The addition of a red fluorescent UAS responder cassette in the same donor plasmid aimed to speed up the testing of UAS/Gal4 combinations in the same G0 animal (instead of creating distinct driver and responder lines that would be much more time consuming). A third donor construct was created lacking the UAS sites upstream of PhA5C to control for GGFF-mediated H2B-mCherry expression (and not direct regulation of the responder cassette by the endogenous *Dll* enhancers) (Figure 27).

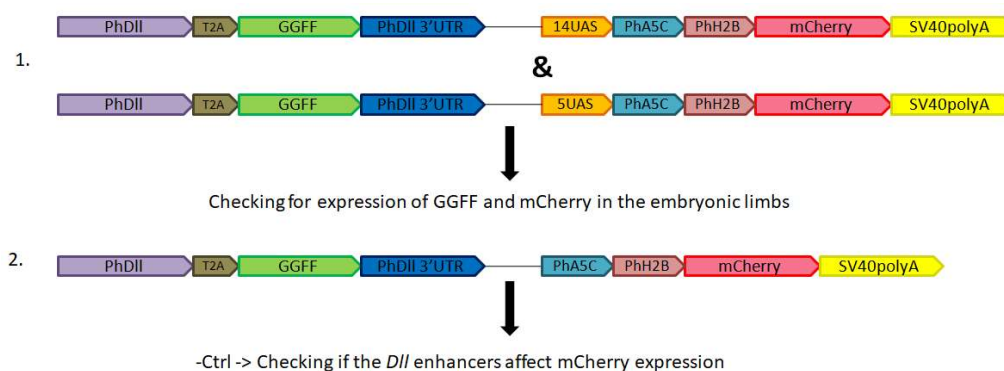
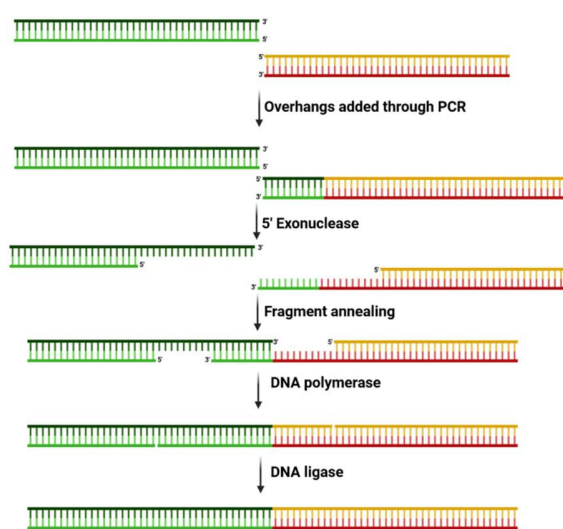


Figure 27: CRISPR NHEJ knock in constructs used in this study to test the Gal4/UAS system in *P.hawaiensis*.

The predominant approach used was that of the T4 ligation cloning, with the exception being the last stage in the creation of the negative control plasmid (pCRISPR-NHEJ-KI-DII-T2A-GGFF-PhA5C-PhH2B-

mCherry) which required the usage of Gibson assembly (due to the inability to find proper restriction digest combinations for conventional cloning). This process involves the fusion of two or more DNA fragments with overlapping ends (added through PCR amplification with primers that had those ends as 5' overhangs) (Figure 28) by the usage of three different enzymes: an exonuclease that removes nucleotides from the 5' ends of DNA fragments to create single-stranded complementary overhangs, a DNA polymerase that fills the gaps present after the hybridization of the fragments and a DNA ligase that closes the remaining nicks (Figure 28). All the previous reactions are done simultaneously in one step leading to the creation of the wanted constructs in less time and with much more accuracy than the conventional ligation protocols.



Created in BioRender.com 

Figure 28: Gibson assembly process. Created in BioRender.com.

Afterwards, the identity of constructed plasmids was verified by different diagnostic restriction digests shown in Figure 29.



Figure 29: (A) Plasmid maps of the CRISPR NHEJ knock in plasmids and **(B)** their respective diagnostic digests. The cutting sites of the used restriction enzymes are shown in each map. In **(B)** the pattern of the used DNA ladder (1Kb+, NEB) is shown on the left for reference and the table on the right indicates the expected patterns for each diagnostic digest.

With the donor plasmids constructed and verified, it was now possible to move on into the generation of the knock in animals. Early 1-cell stage embryos of *P.hawaiensis* were collected and microinjected with one of the three CRISPR knock in mixes. Then the embryos were incubated at 26 °C until they reached stage S20 (112h) to S21 (120h) when appendages are normally almost fully outgrown. At that time, they were screened under a fluorescent stereoscope for the detection of GGFF and mCherry expression in the distal parts of the developing appendages. The results of these experiments are summarized in the following Figure 30:

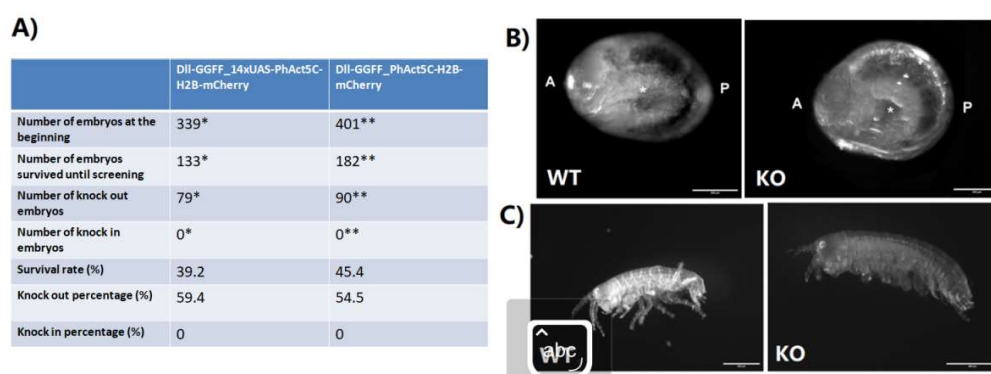


Figure 30: (A) Overview of the microinjection experiments for the creation UAS/Gal4 knock in lines. (*)= Data from 3 independent experiments and (**) = Data from 2 independent experiments. Brightfield images of **(B)** embryos and **(C)** hatchlings exhibiting the wild type (WT) and *DII*/knock out (KO) phenotype. In embryos, A-P denote the anterior-posterior axis, whereas asterisks indicate the embryonic limbs that are truncated in the knock out. Scale bars are at 200µm for embryos and 400µm for hatchlings.

The high rate of knock out phenotypes was an indicator that the Cas9/sgRNA complexes had the expected efficiency. Nevertheless, no GGFF and/or H2B-mCherry fluorescence was detected in any embryo that would be indicative of a knock in event. As an extra control that there was no problem with the protocol or the design of the donor plasmids, I performed an extra CRISPR knock in experiment with the original donor plasmid pCRISPR-NHEJ-KI-DII-T2A-PhH2B-Ruby2 used in Kao et al., 2016. The results from this experiment are presented in Figure 31 below:

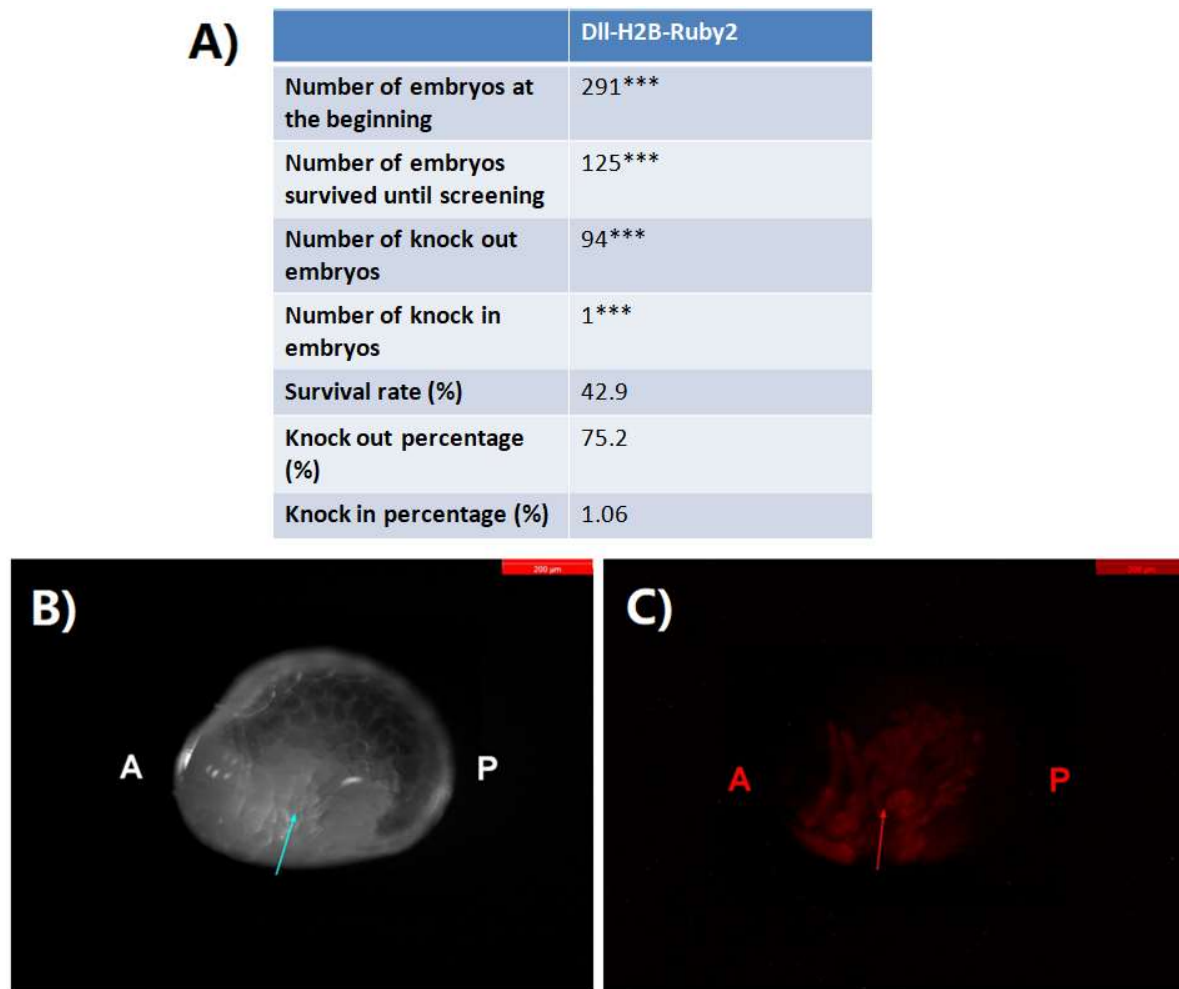


Figure 31: (A) Overview of the microinjection experiments with the H2B-Ruby2 control. (***)= Data from 2 independent experiments. (B) Brightfield and (C) fluorescence images of the knock in embryo. A-P denote the anterior-posterior axis, and the arrow shows the embryonic legs. Scale bars are at 200μm.

These experiments resulted in both the knock out and the knock in phenotypes at the anticipated percentage indicating that the protocol was successful with the used reagents. The expected nuclear localization of the expressed H2B-mRuby2 protein (due to its histone tagging) in distal limb cells was also verified by confocal imaging of the generated knock in G0 embryo (Figure 32).

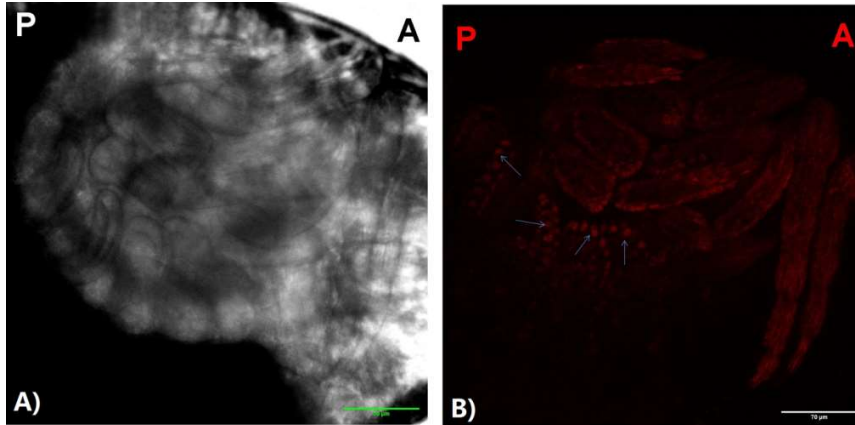


Figure 32: (A) Brightfield and (B) fluorescent confocal images of the knock in embryo. A-P denotes the anterior-posterior axis, whereas arrows in (B) point to individual cell nuclei expressing the fluorescent reporter. Scale bars are at 70μm.

Based on this result, I revisited the G0 embryos that were injected with the UAS/Gal4 constructs (and were kept at -80°C after the screening) but did not show any visible knock in phenotype. Genomic DNA was isolated from the pools of injected embryos that were subjected to PCR to detect any molecular evidence for genomic integration. Using a primer set that specifically hybridized to the genomic template and the integrated plasmid, this PCR analysis would produce a 1450bp band in the case of DII-GGFF-14xUAS_Act5C-H2B-mCherry and a 1100bp band in the case of DII-GGFF_Act5C-H2B-mCherry (Figure 33).

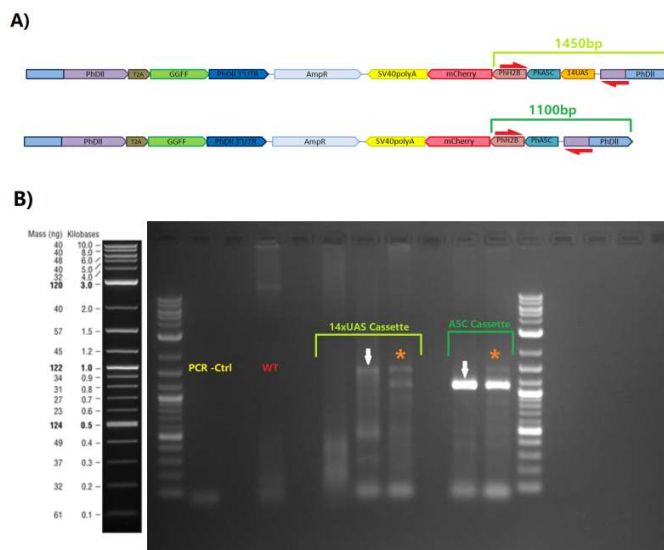


Figure 33: (A) Schematic representation of the knock in-specific PCR fragments. Red arrows indicate the primer binding sites, (B) Genotyping of G0 injected embryos for the detection of knock in events with the UAS/Gal4 constructs. PCR negative control (-ctrl) shows the reaction without template, WT the reaction with genomic DNA template extracted from wild-type uninjected embryos and the rest 5 lanes the reaction with genomic DNA template extracted from pools of embryos injected with the 14xUAS cassette or the basal promoter without the UAS sites. These pattern of the used DNA ladder (1Kb+, NEB) is shown on the left for reference. The white arrows indicate the expected knock in-specific fragments. The asterisks indicate samples that gave additional bands that are characteristic of other UAS/Gal4 cassettes than the expected ones.

Gel electrophoresis revealed the diagnostic bands for CRISPR knock in in 2 out of the 3 pools of embryos injected with the Dll-GGFF-14xUAS_Act5C-H2B-mCherry donor plasmid and in 1 out of the 2 pools of embryos injected with the Dll-GGFF_Act5C-H2B-mCherry donor plasmid. Some additional bands were also detected, especially in the case of Dll-GGFF-14xUAS_Act5C-H2B-mCherry, raising the possibility of truncated knock in events. In any case, the molecular verification of knock in events in injected G0 embryos raises concerns about the absence of GGFF and H2B-mCherry fluorescent signals that might be attributed either to out-of-frame insertions, weak undetectable signal or that the UAS/Gal4 system is nonfunctional. Injection of a larger pool of embryos and further molecular analyses (e.g. sequencing of knock in events) in the future will help resolve this issue.

5. General Conclusions

Both CRISPR knock in experimental approaches used in this thesis didn't result in the desired genetic modifications in any of the two studied emerging model species. This can be attributed either to the relatively small number of animals assayed to recover rare knock in events or to specific problems associated with each project.

In the case of *Tribolium castaneum* CRISPR knock in, it will be important to verify that the very low survival rate is not caused by the disruption of the function of these two targeted genes or any other factor related to the in vivo cutting efficiency of the sgRNAs used or the ssODN templates. In the case of the UAS/Gal4 project in *Parhyale hawaiensis*, the microinjection of more embryos is needed to reach safe conclusions. If knock in events are still detected molecularly but not phenotypically, then testing different combinations of UAS/Gal4 variants (such as the Gal4 and Gal4GFY which have been previously examined) and brighter fluorescent reporters may provide better clues about the functionality of binary expression systems in *Parhyale*.

6. Materials and Methods

Microinjection procedure and laboratory culture maintenance on *Tribolium castaneum*

Tribolium castaneum cultures were maintained in glass food containers with sieved organic whole-wheat flour supplemented with yeast extract (in a ratio 20:1) at 32°C. The food substrate was changed weekly and every 2 months the cultures were renewed in order to avoid any drop in fecundity.

For the microinjection procedure, selected cultures were placed into sieved white wheat flour (type 405) supplemented with yeast extract (again in a ratio 20:1) and left to lay eggs for about 30 min. Then the substrate was passed through a μm sieve in order to separate the eggs. This first batch was thrown away (because the first laid embryos are asynchronous in their development) and the animals were placed again in the white flour substrate to lay eggs for another 2 hours. The eggs isolated this time were kept and placed into Petri dish for aging (because they are too sensitive when freshly laid). Afterwards they were dechorionated with 0.5% bleach solution and aligned into microscope glass cover slips (around 25 embryos per cover slip). Then they were covered with a small sheet of halocarbon oil and placed into a microscope slide in order to be injected. The embryos were injected into their posterior end with an Eppendorf Femtojet 4i Microinjector using borosilicate needles (created in a Sutter Puller Model P-87). The injection mix for the CRISPR gene editing experiments on *T. castaneum* contained 400 ng/ μl Cas9, 100 ng/ μl sgRNA, 100 ng/ μl ssODN (in knock in injections) and 0.05% phenol red dye. Each cover slip with injected embryos was placed into agar juice plates (3% agar, 25% cherry juice and 0.15% Nipagin) at 32°C in order to develop. About a day before their expected hatching they were removed with a small paintbrush and placed into a Watman paper to absorb the halocarbon oil. The paper was then placed again into the agar juice plates at 32°C, which were left open at that stage in order for the vitelline envelope to dry and harden (otherwise the larvae will be unable to pierce through the eggshell and they will die). After their hatching, the first instar larvae were placed into a *Drosophila* culture tubes with whole-wheat flour substrate and left to develop until pupation where they were separated according to their respective sex and placed into different culture tubes. This is done in order to make sure that the female beetles will not mate prematurely as they are able to store sperm into their spermatheca which can be troublesome during crosses.

Crosses were performed by placing each G0 individual with a (3 males for each G0 female and 4 females for each G0 male) into *Drosophila* culture tubes with a very thin sheet of whole-wheat flour substrate and a pinch of bulgur grains (to help the beetle turn back to their feet in case they fall on their backs). Tubes were kept at 32°C and checked weekly for the presence of larvae in the flour.

Microinjection procedure and laboratory culture maintenance on *Parhyale hawaiiensis*

Parhyale hawaiiensis cultures are maintained in plastic containers with artificial sea water (ASW) and crushed coral aquarium substrate at 26°C. Each culture was fed twice a week with a scoop of fish food mixture (44.4% tropical fish flakes, 33.3% wheat germ pellets and 22.2% spirulina flakes) with the addition of a nutrient food supplement (Selcon Vitamin Fish Food Supplement (American Marine Inc))

and Marine Zoe Vitamin Supplement (Kent Marine)) once a week. The ASW in the cultures was changed at weekly basis or earlier if it was necessary (due to the accumulation of dirt and excrements).

For the microinjection procedure, mating pairs were collected a day before the injection and placed into large Petri dishes with ASW. In the next morning, all the released gravid females present in the dishes were anesthetized with CO₂ gas and had their embryos collected with the help of two dissecting forceps. Only those that are in the single cell stage are suitable to be used for the microinjection procedure. The injections were performed in an Eppendorf FemtoJet 5247 Microinjector using borosilicate needles (created in a Sutter Puller Model P-87), by placing a few embryos at a time in 2% agarose step covered in a thin film of sea water under a dissecting microscope. The injection mix for the CRISPR gene editing experiments on *P.hawaiiensis* contained 400ng/μl Cas9, 40ng/μl sgRNA, 10ng/μl donor plasmid and 0.05% phenol red dye. After the microinjection, the embryos were placed into Petri dishes with filtered artificial sea water that contained 25 IU/ml penicillin, 25μg/ml streptomycin and 1.25 μg/ml amphotericin B (a sea water solution known as FASWA) and incubated at 26°C. FASWA changes on the injected embryos were done a daily basis until the hatching of the juveniles.

In vitro transcription of sgRNA

For the in vitro transcription of the needed sgRNAs, the HiScribe T7 High Yield RNA Synthesis Kit (NEB) was used. Firstly, the template DNA molecules that encode each sgRNA had to be synthesized. This is done by PCR amplification using a pair of long primers with overlapping regions. These primers will anneal together during the PCR condition, resulting in the synthesis of desired template DNA molecules with the need of additional substrate. In this case, 3 different primer pairs was used for each the required sgRNA: 1) PhDII_For (5'-GAAATTAATACGACTCACTATAGGCTTCCCCGCCGCGCCATGTAGTTTTAGAGCTAGAAATAGC-3') and PhDII_Rev(5'-AAAAGCACCGACTCGGTGCCACTTTTTCAAGTTGATAACGGACTAGCCTTATTTAACTTGCTATTCTAGCTCTAAAAC-3') for the *Dll*-targeting sgRNA of *P.hawaiiensis*, 2) Tcastaneum_sgRNA_dld_F (5'-GAAATTAATACGACTCACTATAGGGATTGGTCGTGATTGGGTGTTTAGAGCTAGAAATAGC-3') and Tcastaneum_sgRNA_universal (5'-CAAAATCTGATCTTTATCGTTCAATTTTAT-TCCGATCAGGCAATAGTTGAACCTTTTCACCGTGGCTCAGCCACAAA-3') for the *dld*-targeting sgRNA of *T.castaneum*, 3) Tcastaneum_sgRNA_cytb5_F (5'-GAAATTAATACGACTCACTATAGGGTCCATGATAGC-GTCCAGTGTTTTAGA-GCTAGAAATAGC-3') and Tcastaneum_sgRNA_universal (5'-CAAAATCTGATC-TTTATCGTTCAATTTTATTCGATCAGGCAATAGTTGAACCTTTTCACCGTGGCTCAGCCACAAA-3') for the *Cyt-b5-fad*-targeting sgRNA of *T.castaneum*. Each of the previous forward primers contained the T7 promoter sequence at their 5' end, in order for the templates to be transcribable by the T7 RNA polymerase. Afterwards, a 20μl sgRNA synthesis reaction was set that contained 10mM of each ribonucleotide (ATP, UTP, CTP and GTP), 2μl of 10X Reaction Buffer, 300ng template DNA and 2μl of T7 RNA polymerase mix. The reaction was then incubated at 37°C for 4 hours for the in vitro transcription to occur. Then, 2μl of TURBO DNase (2U/μl, Invitrogen) are added in order to degrade the template DNA in the reaction mixture, so that only the transcribed RNA molecules remain. Next, the reaction is stopped by adding 20μl of 5M ammonium acetate (CH₃COONH₄) nuclease-free solution and the RNA was cleaned by one step phenol/chloroform/isoamyl alcohol extraction and two steps of chloroform extraction. Finally, an equal volume of isopropanol was added in the cleaned solution and it was aliquoted into several eppendorf tubes (30μl each) and stored at -20°C for future use.

Primers for the PCR amplification of *Tcdld*, *TcCyt-b-5-fad* and *PhDII* loci

For the PCR of *dld* and *Cytb-5-fad* templates used in In vitro Cas9 cleavage and mismatch nuclease assays on *Tribolium castaneum*, the generic primer pair Tcas_cytb5_scrng_Fgen(5'-TTGGCAG-TTCCACTTCTCG-3') and Tcas_cytb5_scrng_Rgen(5'-CGTGTAAGTGGCTGCATAAC-3') was used for the amplification of *Cytb-5-fad* and the pair of Tcas_dld_scrng_Fgen (5'-ACCCACAGTTCATGTGTCATTG-3') Tcas_dld_scrng_Rgen (5'-TATACACCCACGTTGAGACAAG-3') for the amplification of *dld*.

On the other hand, for the knock in specific PCR assay on the same loci the Tcas_cytb5_spec_R(5'-CGGTCCATTATTGCATCAAGC-3') and Tcas_dld_spec_F (5'-ACGATGCGGATTAGTGGTCATC-3') were used, paired with the Tcas_cytb5_scrng_Fgen and Tcas_dld_scrng_Rgen primers respectively.

For the knock in specific PCR on the *DII* locus of *Parhyale hawaiiensis* the primer pair of PhDIIe_557_Rev (5'-GACTGGGAGCGTGAGGGTA-3') and PhH2B-Rev1 (5'-CTTGGTGATAGACTTCTGG-3')

In vitro cleavage Cas9 assay

In this protocol, a 10µl reaction was set that contained 150ng Cas9 protein, 100 ng sgRNA, 200ng PCR amplified DNA target and 1µl of NEB Buffer 3.1. The reaction was incubated at 37°C for 1h, followed by heat inactivation of Cas9 protein at 65°C for 10min. Then 4 µg of RNaseA were added (for the degradation of the remaining sgRNA molecules) and the samples are incubated again at 37°C for 15min. Finally, the reaction was stopped by the addition of 1µl of stop solution (30% glycerol, 1% SDS and 250mM EDTA pH 8.0) and incubation at 37°C for another 15min. The samples are then analysed by electrophoresis on an agarose gel.

Mismatch Nuclease Assay

For the performance of this assay, 400ng of PCR amplified DNA sample are placed into a thermocycler in a gradually decreasing temperature program (8 different stages from 95°C-25°C with each differing 10°C from the previous one) in order for possible heteroduplexes to form. Then the process continues with the nuclease reaction which on this case was done with Surveyor Assay Kit (Integrated DNA Technologies). This specific protocol involves the addition of 1µl Surveyor Nuclease S, 1µl Surveyor Enhancer S and 1/10th of the final volume 0.15 M MgCl₂ solution. In this case the last component was substituted with 1/5th of the final volume by Phusion High-Fidelity DNA Polymerase + HF Buffer (which contains MgCl₂), so the volume of the added Surveyor Nuclease S had to be increased at 2µl according to company's given instructions. The reaction was then incubated at 42°C for 60min, followed by its termination by adding 1/10th of the volume stop solution. The samples are then analysed by electrophoresis on an agarose gel.

Genomic DNA isolation

For this procedure, 30-80 animals or embryos are collected on 1.5ml eppendorf tubes and frozen at -80°C for 15min at least. Then, 200µl of Buffer A (100mM Tris-HCl pH 7.5, 100mM EDTA, 100mM NaCl and 0.5% SDS) are added in each tube and the animals are grinded with the help of a disposable tissue grinding pestle. Another 200µl of Buffer A are then added and the grinding of the samples continues

until only the cuticles or eggshells remain. Afterwards the samples are incubated at 65°C for 30min, which is followed by the addition of 800µl Buffer B (1 part 5M CH₃COOK solution: 2.5 parts 6M LiCl solution) and incubation on ice for at least 10min. Then, the samples are centrifuged for 15min (13000 rpm at room temperature) in order of the insoluble debris to precipitate. The resulting supernatant is transferred into new 2ml eppendorf tubes, followed by the addition of 600µl isopropanol. The samples are then centrifuge again for 15min (13000 rpm at 4°C) for the precipitation of the genomic DNA. Finally, the resulting DNA pellets are cleaned with a 70% ethanol wash and resuspended in 150µl nuclease free ddH₂O.

Cloning procedure of the *Parhyale* CRISPR knock in donor plasmids

In the first stage of cloning, pPhActin5c-MiTra-DmHsp70polyA, p5xUAS-PhActin5c-MiTra-DmHsp70polyA and p14xUAS-PhActin5c-MiTra-DmHsp70polyA plasmids were digested with BspHI (cuts at the starting codon of the MiTra gene) and EcoRI (cuts inside MiTra coding sequence and after the DmHsp70polyA element), for the isolation of the respective 3054 bp, 3246bp and 3453 bp fragments. Afterwards the pgtz_phh2b_mch_stop_sv40_attb plasmid was digested with NcoI (which is an isocaudomer of BspHI) and EcoRI in order to isolate the 1370 bp PhH2B-mCherry-SV40polyA cassette. This cassette was cloned into the previously isolated BspHI/EcoRI-digested fragments, replacing MiTra-DmHsp70polyA with PhH2B-mCherry-SV40polyA. This led to the creation of the plasmids pPhA5C-PhH2B-mCherry-SV40polyA, p5xUAS-PhActin5c- PhH2B-mCherry-SV40polyA and p14xUAS-PhActin5c- PhH2B-mCherry-SV40polyA.

The next step was to PCR amplify the GGFF gene from the pMi(3xP3-EGFP-PhMS-GGFF) plasmid with the primers GGFF_NotI_Rev (5'-AATTGCGGCCGCTTAGTTACCCGGGAGCATATCG-3') and GGFF_For(5'-GACAACGGGCTGAGTGACA-3'). Afterwards the PCR product was digested with NcoI (cuts at the starting codon of GGFF) and NotI (introduced by GGFF_NotI_Rev primer) and the resulted 1265bp fragment was cloned into a NotI-linearized and NcoI partial digested pCRISPR_NHEJ_KI_DS3_DII-T2A-H2B-Ruby2 plasmid (4.39kb), in which it replaced the H2B-Ruby2 gene and creating the pCRISPR_NHEJ_KI_DS3_DII-T2A-GGFF plasmid.

For the final step, the p14xUAS-PhActin5c-PhH2B-mCherry and p5xUAS-PhActin5c-PhH2B-mCherry plasmids were digested with SphI and SmaI in order to isolate the two UAS cassettes (2.4kb and 2.2kb fragments respectively). These two cassettes were later cloned in a ZraI-linearized and SphI partial digested pCRISPR_NHEJ_KI_DS3_DII-T2A-GGFF plasmid (5.65kb) in order to create the two final donor plasmids pCRISPR_NHEJ_KI_DS3_DII-T2A-GGFF-14xUAS-PhA5C-PhH2B-mCherry-SV40 and pCRISPR_NHEJ_KI_DS3_DII-T2A-GGFF-5xUAS-PhA5C-PhH2B-mCherry-SV40.

The creation of the control plasmid pCRISPR_NHEJ_KI_DS3_DII-T2A-GGFF-PhA5C-PhH2B-mCherry-SV40 control was performed with Gibson assembly through the use of the NEBuilder HiFi DNA Assembly Cloning Kit (NEB). More specifically, the PhA5C-PhH2B-mCherry cassette was PCR amplified with the GBS_Zra_SV40_F (5'-CGAATTGGGCCCCGACGGGCTGCAGGAATTCCAG-3') and GBS_Zra_UAS-Act_R (5'-GGGGAAGCCGCATGCGACATCCCCACCGGAATTGCG-3') primers and mixed with a ZraI-linearized pCRISPR_NHEJ_KI_DS3_DII-T2A-GGFF vector in a 2:1 ratio. Then, an equal volume of 2XNEBuilderHiFi

DNA Assembly Master Mix was added followed by an incubation of the mixture at 50°C for 15min for the reaction to take place.

At the end of each cloning reaction, the samples were transformed into DH5a competent cells (efficiency = 2×10^7 cfu/ μ g pUC19 DNA) in order to screen for positive clones. Bacteria were grown in LB plates containing either kanamycin (50 μ g/ml) or ampicillin (100 μ g/ml) depending on the selection gene on the plasmid and the isolation of plasmid DNA was done with the alkaline lysis protocol.

7. References

- Adams, K.L., Sawadogo, S.P., Nignan, C., Niang, A., Paton, D.G., Robert Shaw, W., South, A., Wang, J., Itoe, M.A., Werling, K., Dabiré, R.K., Diabaté, A., Catteruccia, F., 2021. Cuticular hydrocarbons are associated with mating success and insecticide resistance in malaria vectors. *Commun. Biol.* 4, 1–8. <https://doi.org/10.1038/s42003-021-02434-1>
- Akitake, C.M., Macurak, M., Halpern, M.E., Goll, M.G., 2011. Transgenerational analysis of transcriptional silencing in zebrafish. *Dev. Biol.* 352, 191–201. <https://doi.org/10.1016/j.ydbio.2011.01.002>
- Anders, C., Niewoehner, O., Duerst, A., Jinek, M., 2014. Structural basis of PAM-dependent target DNA recognition by the Cas9 endonuclease. *Nature* 513, 569–573. <https://doi.org/10.1038/nature13579>
- Anzalone, A.V., Randolph, P.B., Davis, J.R., Sousa, A.A., Koblan, L.W., Levy, J.M., Chen, P.J., Wilson, C., Newby, G.A., Raguram, A., Liu, D.R., 2019. Search-and-replace genome editing without double-strand breaks or donor DNA. *Nature* 576, 149–157. <https://doi.org/10.1038/s41586-019-1711-4>
- Arbuthnot, P., 2015. Chapter 3 - Engineering Sequence-Specific DNA Binding Proteins for Antiviral Gene Editing, in: Arbuthnot, P. (Ed.), *Gene Therapy for Viral Infections*. Academic Press, Amsterdam, pp. 63–94. <https://doi.org/10.1016/B978-0-12-410518-8.00003-X>
- Archontidis Themis, A.T., 2020. Establishment of binary expression systems in the amphipod crustacean *Parhyale hawaiiensis* (Bachelor Thesis). University of Crete.
- Armstrong, G.A.B., Liao, M., You, Z., Lissouba, A., Chen, B.E., Drapeau, P., 2016. Homology Directed Knockin of Point Mutations in the Zebrafish *tardbp* and *fus* Genes in ALS Using the CRISPR/Cas9 System. *PLOS ONE* 11, e0150188. <https://doi.org/10.1371/journal.pone.0150188>
- Asakawa, K., Suster, M.L., Mizusawa, K., Nagayoshi, S., Kotani, T., Urasaki, A., Kishimoto, Y., Hibi, M., Kawakami, K., 2008. Genetic dissection of neural circuits by Tol2 transposon-mediated Gal4 gene and enhancer trapping in zebrafish. *Proc. Natl. Acad. Sci.* 105, 1255–1260. <https://doi.org/10.1073/pnas.0704963105>
- Auer, T.O., Duroure, K., Cian, A.D., Concordet, J.-P., Bene, F.D., 2014. Highly efficient CRISPR/Cas9-mediated knock-in in zebrafish by homology-independent DNA repair. *Genome Res.* 24, 142–153. <https://doi.org/10.1101/gr.161638.113>
- Aumann, R.A., Schetelig, M.F., Häcker, I., 2018. Highly efficient genome editing by homology-directed repair using Cas9 protein in *Ceratitis capitata*. *Insect Biochem. Mol. Biol.* 101, 85–93. <https://doi.org/10.1016/j.ibmb.2018.08.004>
- Averof, M., Akam, M., 1995. Hox genes and the diversification of insect and crustacean body plans. *Nature* 376, 420–423. <https://doi.org/10.1038/376420a0>
- Balabanidou, V., Grigoraki, L., Vontas, J., 2018. Insect cuticle: a critical determinant of insecticide resistance. *Curr. Opin. Insect Sci., Pests and resistance * Behavioural ecology* 27, 68–74. <https://doi.org/10.1016/j.cois.2018.03.001>
- Baron, U., Gossen, M., Bujard, H., 1997. Tetracycline-controlled transcription in eukaryotes: novel transactivators with graded transactivation potential. *Nucleic Acids Res.* 25, 2723–2729.
- Barrangou, R., Fremaux, C., Deveau, H., Richards, M., Boyaval, P., Moineau, S., Romero, D.A., Horvath, P., 2007. CRISPR Provides Acquired Resistance Against Viruses in Prokaryotes. *Science* 315, 1709–1712. <https://doi.org/10.1126/science.1138140>
- Beermann, A., Aranda, M., Schröder, R., 2004. The Sp8 zinc-finger transcription factor is involved in allometric growth of the limbs in the beetle *Tribolium castaneum*. *Dev. Camb. Engl.* 131, 733–742. <https://doi.org/10.1242/dev.00974>

- Bell, C.H., 2014. 15 - Pest control of stored food products: insects and mites, in: Lelieveld, H.L.M., Holah, J.T., Napper, D. (Eds.), *Hygiene in Food Processing (Second Edition)*, Woodhead Publishing Series in Food Science, Technology and Nutrition. Woodhead Publishing, pp. 494–538.
<https://doi.org/10.1533/9780857098634.3.494>
- Benton, M.A., Akam, M., Pavlopoulos, A., 2013. Cell and tissue dynamics during *Tribolium* embryogenesis revealed by versatile fluorescence labeling approaches. *Dev. Camb. Engl.* 140, 3210–3220. <https://doi.org/10.1242/dev.096271>
- Berg, J.M., Tymoczko, J.L., Jr, G.J.G., Stryer, L., 2015. *Biochemistry*, Eighth edition. ed. W. H. Freeman, New York.
- Bitinaite, J., Wah, D.A., Aggarwal, A.K., Schildkraut, I., 1998. FokI dimerization is required for DNA cleavage. *Proc. Natl. Acad. Sci.* 95, 10570–10575. <https://doi.org/10.1073/pnas.95.18.10570>
- Boel, A., De Saffel, H., Steyaert, W., Callewaert, B., De Paepe, A., Coucke, P.J., Willaert, A., 2018. CRISPR/Cas9-mediated homology-directed repair by ssODNs in zebrafish induces complex mutational patterns resulting from genomic integration of repair-template fragments. *Dis. Model. Mech.* 11, dmm035352. <https://doi.org/10.1242/dmm.035352>
- Bolotin, A., Quinquis, B., Sorokin, A., Ehrlich, S.D., 2005. Clustered regularly interspaced short palindrome repeats (CRISPRs) have spacers of extrachromosomal origin. *Microbiology* 151, 2551–2561. <https://doi.org/10.1099/mic.0.28048-0>
- Bolter, C.J., Chefurka, W., 1990. Extramitochondrial release of hydrogen peroxide from insect and mouse liver mitochondria using the respiratory inhibitors phosphine, myxothiazol, and antimycin and spectral analysis of inhibited cytochromes. *Arch. Biochem. Biophys.* 278, 65–72.
[https://doi.org/10.1016/0003-9861\(90\)90232-n](https://doi.org/10.1016/0003-9861(90)90232-n)
- Bosch, J.A., Colbeth, R., Zirin, J., Perrimon, N., 2020. Gene Knock-Ins in *Drosophila* Using Homology-Independent Insertion of Universal Donor Plasmids. *Genetics* 214, 75–89.
<https://doi.org/10.1534/genetics.119.302819>
- Boutet, A., Schierwater, B. (Eds.), 2022. *Handbook of Marine Model Organisms in Experimental Biology: Established and Emerging*. Taylor & Francis. <https://doi.org/10.1201/9781003217503>
- Brand, A.H., Perrimon, N., 1993. Targeted gene expression as a means of altering cell fates and generating dominant phenotypes. *Dev. Camb. Engl.* 118, 401–415.
<https://doi.org/10.1242/dev.118.2.401>
- Brouns, S.J.J., Jore, M.M., Lundgren, M., Westra, E.R., Slijkhuys, R.J.H., Snijders, A.P.L., Dickman, M.J., Makarova, K.S., Koonin, E.V., van der Oost, J., 2008. Small CRISPR RNAs Guide Antiviral Defense in Prokaryotes. *Science* 321, 960–964. <https://doi.org/10.1126/science.1159689>
- Brown, S.J., Shippy, T.D., Miller, S., Bolognesi, R., Beeman, R.W., Lorenzen, M.D., Bucher, G., Wimmer, E.A., Klingler, M., 2009. The Red Flour Beetle, *Tribolium castaneum* (Coleoptera): A Model for Studies of Development and Pest Biology. *Cold Spring Harb. Protoc.* 2009, pdb.emo126.
<https://doi.org/10.1101/pdb.emo126>
- Browne, W.E., Price, A.L., Gerberding, M., Patel, N.H., 2005. Stages of embryonic development in the amphipod crustacean, *Parhyale hawaiiensis*. *Genes. N. Y. N* 2000 42, 124–149.
<https://doi.org/10.1002/gene.20145>
- Burt, A., Koufopanou, V., 2004. Homing endonuclease genes: the rise and fall and rise again of a selfish element. *Curr. Opin. Genet. Dev.* 14, 609–615. <https://doi.org/10.1016/j.gde.2004.09.010>
- Campbell, J.F., Athanassiou, C.G., Hagstrum, D.W., Zhu, K.Y., 2022. *Tribolium castaneum*: A Model Insect for Fundamental and Applied Research. *Annu. Rev. Entomol.* 67, 347–365.
<https://doi.org/10.1146/annurev-ento-080921-075157>
- Carini, M., Aldini, G., Facino, R.M., 2004. Mass spectrometry for detection of 4-hydroxy-trans-2-nonenal (HNE) adducts with peptides and proteins. *Mass Spectrom. Rev.* 23, 281–305.
<https://doi.org/10.1002/mas.10076>

- Carothers, D.J., Pons, G., Patel, M.S., 1989. Dihydrolipoamide dehydrogenase: functional similarities and divergent evolution of the pyridine nucleotide-disulfide oxidoreductases. *Arch. Biochem. Biophys.* 268, 409–425. [https://doi.org/10.1016/0003-9861\(89\)90309-3](https://doi.org/10.1016/0003-9861(89)90309-3)
- Chalkia Georgia, C.G., 2021. Establishment of binary expression UAS/Gal4 in amphipod crustacean *Parhyale hawaiiensis*. University of Crete.
- Chaudhry, M.Q., Price, N.R., 1992. Comparison of the oxidant damage induced by phosphine and the uptake and tracheal exchange of ³²P-radiolabelled phosphine in the susceptible and resistant strains of *Rhyzopertha dominica* (F.) (Coleoptera: Bostrychidae). *Pestic. Biochem. Physiol.* 42, 167–179. [https://doi.org/10.1016/0048-3575\(92\)90063-6](https://doi.org/10.1016/0048-3575(92)90063-6)
- Chen, P.J., Hussmann, J.A., Yan, J., Knipping, F., Ravisankar, P., Chen, P.-F., Chen, C., Nelson, J.W., Newby, G.A., Sahin, M., Osborn, M.J., Weissman, J.S., Adamson, B., Liu, D.R., 2021. Enhanced prime editing systems by manipulating cellular determinants of editing outcomes. *Cell* 184, 5635–5652.e29. <https://doi.org/10.1016/j.cell.2021.09.018>
- Clark, E., Peel, A.D., Akam, M., 2019. Arthropod segmentation. *Dev. Camb. Engl.* 146, dev170480. <https://doi.org/10.1242/dev.170480>
- Colbourne, J.K., Pfrender, M.E., Gilbert, D., Thomas, W.K., Tucker, A., Oakley, T.H., Tokishita, S., Aerts, A., Arnold, G.J., Basu, M.K., Bauer, D.J., Cáceres, C.E., Carmel, L., Casola, C., Choi, J.-H., Detter, J.C., Dong, Q., Dusheyko, S., Eads, B.D., Fröhlich, T., Geiler-Samerotte, K.A., Gerlach, D., Hatcher, P., Jogdeo, S., Krijgsveld, J., Kriventseva, E.V., Kültz, D., Laforsch, C., Lindquist, E., Lopez, J., Manak, J.R., Muller, J., Pangilinan, J., Patwardhan, R.P., Pitluck, S., Pritham, E.J., Rechtsteiner, A., Rho, M., Rogozin, I.B., Sakarya, O., Salamov, A., Schaack, S., Shapiro, H., Shiga, Y., Skalitzy, C., Smith, Z., Souvorov, A., Sung, W., Tang, Z., Tsuchiya, D., Tu, H., Vos, H., Wang, M., Wolf, Y.I., Yamagata, H., Yamada, T., Ye, Y., Shaw, J.R., Andrews, J., Crease, T.J., Tang, H., Lucas, S.M., Robertson, H.M., Bork, P., Koonin, E.V., Zdobnov, E.M., Grigoriev, I.V., Lynch, M., Boore, J.L., 2011. The Ecoresponsive Genome of *Daphnia pulex*. *Science* 331, 555–561. <https://doi.org/10.1126/science.1197761>
- Copf, T., Schröder, R., Averof, M., 2004. Ancestral role of caudal genes in axis elongation and segmentation. *Proc. Natl. Acad. Sci.* 101, 17711–17715. <https://doi.org/10.1073/pnas.0407327102>
- Deltcheva, E., Chylinski, K., Sharma, C.M., Gonzales, K., Chao, Y., Pirzada, Z.A., Eckert, M.R., Vogel, J., Charpentier, E., 2011. CRISPR RNA maturation by trans-encoded small RNA and host factor RNase III. *Nature* 471, 602–607. <https://doi.org/10.1038/nature09886>
- Denes, C.E., Cole, A.J., Aksoy, Y.A., Li, G., Neely, G.G., Hesselson, D., 2021. Approaches to Enhance Precise CRISPR/Cas9-Mediated Genome Editing. *Int. J. Mol. Sci.* 22, 8571. <https://doi.org/10.3390/ijms22168571>
- Deshmukh, S., Ponnaluri, V.C., Dai, N., Pradhan, S., Deobagkar, D., 2018. Levels of DNA cytosine methylation in the *Drosophila* genome. *PeerJ* 6, e5119. <https://doi.org/10.7717/peerj.5119>
- Deveau, H., Barrangou, R., Garneau, J.E., Labonté, J., Fremaux, C., Boyaval, P., Romero, D.A., Horvath, P., Moineau, S., 2008. Phage Response to CRISPR-Encoded Resistance in *Streptococcus thermophilus*. *J. Bacteriol.* 190, 1390–1400. <https://doi.org/10.1128/JB.01412-07>
- Dong, P.D.S., Chu, J., Panganiban, G., 2001. Proximodistal domain specification and interactions in developing *Drosophila* appendages. *Development* 128, 2365–2372. <https://doi.org/10.1242/dev.128.12.2365>
- Donnelly, M.L.L., Hughes, L.E., Luke, G., Mendoza, H., ten Dam, E., Gani, D., Ryan, M.D., 2001a. The ‘cleavage’ activities of foot-and-mouth disease virus 2A site-directed mutants and naturally occurring ‘2A-like’ sequences. *J. Gen. Virol.* 82, 1027–1041. <https://doi.org/10.1099/0022-1317-82-5-1027>

- Donnelly, M.L.L., Luke, G., Mehrotra, A., Li, X., Hughes, L.E., Gani, D., Ryan, M.D., 2001b. Analysis of the aphthovirus 2A/2B polyprotein 'cleavage' mechanism indicates not a proteolytic reaction, but a novel translational effect: a putative ribosomal 'skip.' *J. Gen. Virol.* 82, 1013–1025. <https://doi.org/10.1099/0022-1317-82-5-1013>
- Duffy, J.B., 2002. GAL4 system in *Drosophila*: a fly geneticist's Swiss army knife. *Genes. N. Y.* N 2000 34, 1–15. <https://doi.org/10.1002/gene.10150>
- Elliott, D.A., Brand, A.H., 2008. The GAL4 system : a versatile system for the expression of genes. *Methods Mol. Biol.* Clifton NJ 420, 79–95. https://doi.org/10.1007/978-1-59745-583-1_5
- Encyclopedia of Animal Behavior [WWW Document], n.d. . ScienceDirect. URL <http://www.sciencedirect.com:5070/referencework/9780128132524/encyclopedia-of-animal-behavior> (accessed 3.12.23).
- Estella, C., Voutev, R., Mann, R.S., 2012. A dynamic network of morphogens and transcription factors patterns the fly leg. *Curr. Top. Dev. Biol.* 98, 173–198. <https://doi.org/10.1016/B978-0-12-386499-4.00007-0>
- Feyereisen, R., 1995. Molecular biology of insecticide resistance. *Toxicol. Lett.*, Proceedings of the International Congress of Toxicology - VII 82–83, 83–90. [https://doi.org/10.1016/0378-4274\(95\)03470-6](https://doi.org/10.1016/0378-4274(95)03470-6)
- Garneau, J.E., Dupuis, M.-È., Villion, M., Romero, D.A., Barrangou, R., Boyaval, P., Fremaux, C., Horvath, P., Magadán, A.H., Moineau, S., 2010. The CRISPR/Cas bacterial immune system cleaves bacteriophage and plasmid DNA. *Nature* 468, 67–71. <https://doi.org/10.1038/nature09523>
- Gill, G., Ptashne, M., 1988. Negative effect of the transcriptional activator GAL4. *Nature* 334, 721–724. <https://doi.org/10.1038/334721a0>
- Gilles, A.F., Schinko, J.B., Averof, M., 2015. Efficient CRISPR-mediated gene targeting and transgene replacement in the beetle *Tribolium castaneum*. *Development* 142, 2832–2839. <https://doi.org/10.1242/dev.125054>
- González Castro, N., Bjelic, J., Malhotra, G., Huang, C., Alsaffar, S.H., 2021. Comparison of the Feasibility, Efficiency, and Safety of Genome Editing Technologies. *Int. J. Mol. Sci.* 22, 10355. <https://doi.org/10.3390/ijms221910355>
- Grabher, C., Wittbrodt, J., 2004. Efficient activation of gene expression using a heat-shock inducible Gal4/Vp16-UAS system in medaka. *BMC Biotechnol.* 4, 26. <https://doi.org/10.1186/1472-6750-4-26>
- Gratz, S.J., Rubinstein, C.D., Harrison, M.M., Wildonger, J., O'Connor-Giles, K.M., 2015. CRISPR-Cas9 Genome Editing in *Drosophila*. *Curr. Protoc. Mol. Biol.* 111, 31.2.1–31.2.20. <https://doi.org/10.1002/0471142727.mb3102s111>
- Gratz, S.J., Uken, F.P., Rubinstein, C.D., Thiede, G., Donohue, L.K., Cummings, A.M., O'Connor-Giles, K.M., 2014. Highly Specific and Efficient CRISPR/Cas9-Catalyzed Homology-Directed Repair in *Drosophila*. *Genetics* 196, 961–971. <https://doi.org/10.1534/genetics.113.160713>
- Hale, C.R., Zhao, P., Olson, S., Duff, M.O., Graveley, B.R., Wells, L., Terns, R.M., Terns, M.P., 2009. RNA-Guided RNA Cleavage by a CRISPR RNA-Cas Protein Complex. *Cell* 139, 945–956. <https://doi.org/10.1016/j.cell.2009.07.040>
- Heryanto, C., Hanly, J.J., Mazo-Vargas, A., Tendolkar, A., Martin, A., 2022. Mapping and CRISPR homology-directed repair of a recessive white eye mutation in *Plodia* moths. *iScience* 25, 103885. <https://doi.org/10.1016/j.isci.2022.103885>
- Horn, C., Offen, N., Nystedt, S., Häcker, U., Wimmer, E.A., 2003. piggyBac-based insertional mutagenesis and enhancer detection as a tool for functional insect genomics. *Genetics* 163, 647–661. <https://doi.org/10.1093/genetics/163.2.647>
- Hsu, P.D., Lander, E.S., Zhang, F., 2014. Development and Applications of CRISPR-Cas9 for Genome Engineering. *Cell* 157, 1262–1278. <https://doi.org/10.1016/j.cell.2014.05.010>

- Humphries, K.M., Szveda, L.I., 1998. Selective inactivation of alpha-ketoglutarate dehydrogenase and pyruvate dehydrogenase: reaction of lipoic acid with 4-hydroxy-2-nonenal. *Biochemistry* 37, 15835–15841. <https://doi.org/10.1021/bi981512h>
- Hwang, W.Y., Fu, Y., Reyon, D., Maeder, M.L., Kaini, P., Sander, J.D., Joung, J.K., Peterson, R.T., Yeh, J.-R.J., 2013. Heritable and Precise Zebrafish Genome Editing Using a CRISPR-Cas System. *PLOS ONE* 8, e68708. <https://doi.org/10.1371/journal.pone.0068708>
- Inhibition of mitochondrial respiration: HNE inactivation of lipoic acid containing dehydrogenases: Kenneth M. Humphries and Luke I. Szveda. Department of Physiology and Biophysics, School of Medicine, Case Western Reserve University, Cleveland, Ohio, 1998. . *Free Radic. Biol. Med.*, 5th Annual Meeting of the Oxygen Society 25, S84. [https://doi.org/10.1016/S0891-5849\(98\)90265-9](https://doi.org/10.1016/S0891-5849(98)90265-9)
- Irion, U., Krauss, J., Nüsslein-Volhard, C., 2014. Precise and efficient genome editing in zebrafish using the CRISPR/Cas9 system. *Development* 141, 4827–4830. <https://doi.org/10.1242/dev.115584>
- Ishino, Y., Shinagawa, H., Makino, K., Amemura, M., Nakata, A., 1987. Nucleotide sequence of the *iap* gene, responsible for alkaline phosphatase isozyme conversion in *Escherichia coli*, and identification of the gene product. *J. Bacteriol.* 169, 5429–5433. <https://doi.org/10.1128/jb.169.12.5429-5433.1987>
- Jagadeesan, R., Collins, P.J., Daglish, G.J., Ebert, P.R., Schlipalius, D.I., 2012. Phosphine Resistance in the Rust Red Flour Beetle, *Tribolium castaneum* (Coleoptera: Tenebrionidae): Inheritance, Gene Interactions and Fitness Costs. *PLOS ONE* 7, e31582. <https://doi.org/10.1371/journal.pone.0031582>
- Jagadeesan, R., Collins, P.J., Nayak, M.K., Schlipalius, D.I., Ebert, P.R., 2016. Genetic characterization of field-evolved resistance to phosphine in the rusty grain beetle, *Cryptolestes ferrugineus* (Laemophloeidae: Coleoptera). *Pestic. Biochem. Physiol.* 127, 67–75. <https://doi.org/10.1016/j.pestbp.2015.09.008>
- Jagadeesan, R., Schlipalius, D.I., Singarayan, V.T., Nath, N.S., Nayak, M.K., Ebert, P.R., 2021. Unique genetic variants in dihydrolipoamide dehydrogenase (*dld*) gene confer strong resistance to phosphine in the rusty grain beetle, *Cryptolestes ferrugineus* (Stephens). *Pestic. Biochem. Physiol.* 171, 104717. <https://doi.org/10.1016/j.pestbp.2020.104717>
- Jasin, M., 1996. Genetic manipulation of genomes with rare-cutting endonucleases. *Trends Genet.* 12, 224–228. [https://doi.org/10.1016/0168-9525\(96\)10019-6](https://doi.org/10.1016/0168-9525(96)10019-6)
- Ji, Z., Guo, W., Chen, X., Wang, C., Zhao, K., 2022. Plant Executor Genes. *Int. J. Mol. Sci.* 23, 1524. <https://doi.org/10.3390/ijms23031524>
- Jinek, M., Chylinski, K., Fonfara, I., Hauer, M., Doudna, J.A., Charpentier, E., 2012. A Programmable Dual-RNA-Guided DNA Endonuclease in Adaptive Bacterial Immunity. *Science* 337, 816–821. <https://doi.org/10.1126/science.1225829>
- Kakidani, H., Ptashne, M., 1988. GAL4 activates gene expression in mammalian cells. *Cell* 52, 161–167. [https://doi.org/10.1016/0092-8674\(88\)90504-1](https://doi.org/10.1016/0092-8674(88)90504-1)
- Kao, D., Lai, A.G., Stamatakis, E., Rosic, S., Konstantinides, N., Jarvis, E., Di Donfrancesco, A., Pouchkina-Stancheva, N., Sémon, M., Grillo, M., Bruce, H., Kumar, S., Siwanowicz, I., Le, A., Lemire, A., Eisen, M.B., Extavour, C., Browne, W.E., Wolff, C., Averof, M., Patel, N.H., Sarkies, P., Pavlopoulos, A., Aboobaker, A., 2016. The genome of the crustacean *Parhyale hawaiiensis*, a model for animal development, regeneration, immunity and lignocellulose digestion. *eLife* 5, e20062. <https://doi.org/10.7554/eLife.20062>
- Kaplan, P., Tatarkova, Z., Racay, P., Lehotsky, J., Pavlikova, M., Dobrota, D., 2007. Oxidative modifications of cardiac mitochondria and inhibition of cytochrome c oxidase activity by 4-hydroxynonenal. *Redox Rep. Commun. Free Radic. Res.* 12, 211–218. <https://doi.org/10.1179/135100007X200308>

- Kaur, R., Subbarayalu, M., Jagadeesan, R., Daglish, G.J., Nayak, M.K., Naik, H.R., Ramasamy, S., Subramanian, C., Ebert, P.R., Schlup, D.I., 2015. Phosphine resistance in India is characterised by a dihydrolipoamide dehydrogenase variant that is otherwise unobserved in eukaryotes. *Heredity* 115, 188–194. <https://doi.org/10.1038/hdy.2015.24>
- Kikuchi, G., Motokawa, Y., Yoshida, T., Hiraga, K., 2008. Glycine cleavage system: reaction mechanism, physiological significance, and hyperglycinemia. *Proc. Jpn. Acad. Ser. B Phys. Biol. Sci.* 84, 246–263. <https://doi.org/10.2183/pjab.84.246>
- Klingler, M., Bucher, G., 2022. The red flour beetle *T. castaneum*: elaborate genetic toolkit and unbiased large scale RNAi screening to study insect biology and evolution. *EvoDevo* 13, 14. <https://doi.org/10.1186/s13227-022-00201-9>
- Kontarakis, Z., Pavlopoulos, A., 2014. Transgenesis in non-model organisms: the case of *Parhyale*. *Methods Mol. Biol.* Clifton NJ 1196, 145–181. https://doi.org/10.1007/978-1-4939-1242-1_10
- Kontarakis, Z., Pavlopoulos, A., Kiupakis, A., Konstantinides, N., Douris, V., Averof, M., 2011. A versatile strategy for gene trapping and trap conversion in emerging model organisms. *Development* 138, 2625–2630. <https://doi.org/10.1242/dev.066324>
- Kumagai, H., Nakanishi, T., Matsuura, T., Kato, Y., Watanabe, H., 2017. CRISPR/Cas-mediated knock-in via non-homologous end-joining in the crustacean *Daphnia magna*. *PLOS ONE* 12, e0186112. <https://doi.org/10.1371/journal.pone.0186112>
- Levi, T., Sloutskin, A., Kalifa, R., Juven-Gershon, T., Gerlitz, O., 2020. Efficient In Vivo Introduction of Point Mutations Using ssODN and a Co-CRISPR Approach. *Biol. Proced. Online* 22, 14. <https://doi.org/10.1186/s12575-020-00123-7>
- Liu, T., Li, L., Zhang, F., Wang, Y., 2015. Transcriptional inhibition of the Catalase gene in phosphine-induced oxidative stress in *Drosophila melanogaster*. *Pestic. Biochem. Physiol.* 124, 1–7. <https://doi.org/10.1016/j.pestbp.2015.05.005>
- Liu, Z., Chen, O., Wall, J.B.J., Zheng, M., Zhou, Y., Wang, L., Ruth Vaseghi, H., Qian, L., Liu, J., 2017. Systematic comparison of 2A peptides for cloning multi-genes in a polycistronic vector. *Sci. Rep.* 7, 2193. <https://doi.org/10.1038/s41598-017-02460-2>
- Liubicich, D.M., Serano, J.M., Pavlopoulos, A., Kontarakis, Z., Protas, M.E., Kwan, E., Chatterjee, S., Tran, K.D., Averof, M., Patel, N.H., 2009. Knockdown of *Parhyale* Ultrabithorax recapitulates evolutionary changes in crustacean appendage morphology. *Proc. Natl. Acad. Sci.* 106, 13892–13896. <https://doi.org/10.1073/pnas.0903105106>
- Lorenzen, M.D., Berghammer, A.J., Brown, S.J., Denell, R.E., Klingler, M., Beeman, R.W., 2003. piggyBac-mediated germline transformation in the beetle *Tribolium castaneum*. *Insect Mol. Biol.* 12, 433–440. <https://doi.org/10.1046/j.1365-2583.2003.00427.x>
- Lycett, G.J., Amenya, D., Lynd, A., 2012. The *Anopheles gambiae* alpha-tubulin-1b promoter directs neuronal, testes and developing imaginal tissue specific expression and is a sensitive enhancer detector. *Insect Mol. Biol.* 21, 79–88. <https://doi.org/10.1111/j.1365-2583.2011.01112.x>
- Lynd, A., Lycett, G.J., 2011. Optimization of the Gal4-UAS system in an *Anopheles gambiae* cell line. *Insect Mol. Biol.* 20, 599–608. <https://doi.org/10.1111/j.1365-2583.2011.01090.x>
- Ma, J., Ptashne, M., 1987. Deletion analysis of GAL4 defines two transcriptional activating segments. *Cell* 48, 847–853. [https://doi.org/10.1016/0092-8674\(87\)90081-x](https://doi.org/10.1016/0092-8674(87)90081-x)
- Marraffini, L.A., Sontheimer, E.J., 2008. CRISPR Interference Limits Horizontal Gene Transfer in *Staphylococci* by Targeting DNA. *Science* 322, 1843–1845. <https://doi.org/10.1126/science.1165771>
- Mojica, F.J.M., Díez-Villaseñor, C., García-Martínez, J., Soria, E., 2005. Intervening Sequences of Regularly Spaced Prokaryotic Repeats Derive from Foreign Genetic Elements. *J. Mol. Evol.* 60, 174–182. <https://doi.org/10.1007/s00239-004-0046-3>

- Mojica, F.J.M., Díez-Villaseñor, C., Soria, E., Juez, G., 2000. Biological significance of a family of regularly spaced repeats in the genomes of Archaea, Bacteria and mitochondria. *Mol. Microbiol.* 36, 244–246. <https://doi.org/10.1046/j.1365-2958.2000.01838.x>
- Montella, I.R., Schama, R., Valle, D., 2012. The classification of esterases: an important gene family involved in insecticide resistance - A review. *Mem. Inst. Oswaldo Cruz* 107, 437–449. <https://doi.org/10.1590/S0074-02762012000400001>
- Nast, A.R., Extavour, C.G., 2014. Ablation of a Single Cell From Eight-cell Embryos of the Amphipod Crustacean *Parhyale hawaiiensis*. *J. Vis. Exp. JoVE* 51073. <https://doi.org/10.3791/51073>
- Nath, N.S., Bhattacharya, I., Tuck, A.G., Schlipalius, D.I., Ebert, P.R., 2011. Mechanisms of Phosphine Toxicity. *J. Toxicol.* 2011, 494168. <https://doi.org/10.1155/2011/494168>
- Nauen, R., Bass, C., Feyereisen, R., Vontas, J., 2022. The Role of Cytochrome P450s in Insect Toxicology and Resistance. *Annu. Rev. Entomol.* 67, 105–124. <https://doi.org/10.1146/annurev-ento-070621-061328>
- Nguyen, T.T., Collins, P.J., Duong, T.M., Schlipalius, D.I., Ebert, P.R., 2016. Genetic Conservation of Phosphine Resistance in the Rice Weevil *Sitophilus oryzae* (L.). *J. Hered.* 107, 228–237. <https://doi.org/10.1093/jhered/esw001>
- Niu, X., Mi, L., Li, Y., Wei, A., Yang, Z., Wu, J., Zhang, D., Song, X., 2013. Physiological and biochemical responses of rice seeds to phosphine exposure during germination. *Chemosphere* 93, 2239–2244. <https://doi.org/10.1016/j.chemosphere.2013.07.074>
- Özhan-Kizil, G., Havemann, J., Gerberding, M., 2009. Germ cells in the crustacean *Parhyale hawaiiensis* depend on Vasa protein for their maintenance but not for their formation. *Dev. Biol.* 327, 230–239. <https://doi.org/10.1016/j.ydbio.2008.10.028>
- Paris, M., Wolff, C., Patel, N.H., Averof, M., 2022. Chapter Eight - The crustacean model *Parhyale hawaiiensis*, in: Goldstein, B., Srivastava, M. (Eds.), *Current Topics in Developmental Biology, Emerging Model Systems in Developmental Biology*. Academic Press, pp. 199–230. <https://doi.org/10.1016/bs.ctdb.2022.02.001>
- Pavlidis, N., Vontas, J., Van Leeuwen, T., 2018. The role of glutathione S-transferases (GSTs) in insecticide resistance in crop pests and disease vectors. *Curr. Opin. Insect Sci.* 27, 97–102. <https://doi.org/10.1016/j.cois.2018.04.007>
- Pavlopoulos, A., Averof, M., 2005. Establishing genetic transformation for comparative developmental studies in the crustacean *Parhyale hawaiiensis*. *Proc. Natl. Acad. Sci.* 102, 7888–7893. <https://doi.org/10.1073/pnas.0501101102>
- Pavlopoulos, A., Berghammer, A.J., Averof, M., Klingler, M., 2004. Efficient transformation of the beetle *Tribolium castaneum* using the Minos transposable element: quantitative and qualitative analysis of genomic integration events. *Genetics* 167, 737–746. <https://doi.org/10.1534/genetics.103.023085>
- P.C. Annis, A., E., Atkins, C.A., A., G.A., Atwell, W., n.d. *Encyclopedia of Food Grains* [WWW Document]. ScienceDirect. URL <http://www.sciencedirect.com:5070/referencework/9780123947864/encyclopedia-of-food-grains> (accessed 3.12.23).
- Poore, G., 2005. Peracarida: Monophyly, relationships and evolutionary success. *Nauplius* 13, 1–27.
- Pourcel, C., Salvignol, G., Vergnaud, G., 2005. CRISPR elements in *Yersinia pestis* acquire new repeats by preferential uptake of bacteriophage DNA, and provide additional tools for evolutionary studies. *Microbiology* 151, 653–663. <https://doi.org/10.1099/mic.0.27437-0>
- Pringle, F.M., Gordon, K.H., Hanzlik, T.N., Kalmakoff, J., Scotti, P.D., Ward, V.K., 1999. A novel capsid expression strategy for *Thosea asigna* virus (Tetraviridae). *J. Gen. Virol.* 80, 1855–1863. <https://doi.org/10.1099/0022-1317-80-7-1855>

- Quadros, R.M., Miura, H., Harms, D.W., Akatsuka, H., Sato, T., Aida, T., Redder, R., Richardson, G.P., Inagaki, Y., Sakai, D., Buckley, S.M., Seshacharyulu, P., Batra, S.K., Behlke, M.A., Zeiner, S.A., Jacobi, A.M., Izu, Y., Thoreson, W.B., Urness, L.D., Mansour, S.L., Ohtsuka, M., Gurumurthy, C.B., 2017. Easi-CRISPR: a robust method for one-step generation of mice carrying conditional and insertion alleles using long ssDNA donors and CRISPR ribonucleoproteins. *Genome Biol.* 18, 92. <https://doi.org/10.1186/s13059-017-1220-4>
- Rehm, E.J., Hannibal, R.L., Chaw, R.C., Vargas-Vila, M.A., Patel, N.H., 2009. The crustacean *Parhyale hawaiiensis*: a new model for arthropod development. *Cold Spring Harb. Protoc.* 2009, pdb.emo114. <https://doi.org/10.1101/pdb.emo114>
- Riabinina, O., Potter, C.J., 2016. The Q-System: A Versatile Expression System for *Drosophila*. *Methods Mol. Biol. Clifton NJ* 1478, 53–78. https://doi.org/10.1007/978-1-4939-6371-3_3
- Rørth, P., 1996. A modular misexpression screen in *Drosophila* detecting tissue-specific phenotypes. *Proc. Natl. Acad. Sci. U. S. A.* 93, 12418–12422. <https://doi.org/10.1073/pnas.93.22.12418>
- Rösner, J., Wellmeyer, B., Merzendorfer, H., 2020. *Tribolium castaneum*: A Model for Investigating the Mode of Action of Insecticides and Mechanisms of Resistance. *Curr. Pharm. Des.* 26, 3554–3568. <https://doi.org/10.2174/1381612826666200513113140>
- Sadowski, I., Ma, J., Triezenberg, S., Ptashne, M., 1988. GAL4-VP16 is an unusually potent transcriptional activator. *Nature* 335, 563–564. <https://doi.org/10.1038/335563a0>
- Schaeper, N.D., Wimmer, E.A., Prpic, N.-M., 2013. Appendage patterning in the primitively wingless hexapods *Thermobia domestica* (Zygentoma: Lepismatidae) and *Folsomia candida* (Collembola: Isotomidae). *Dev. Genes Evol.* 223, 341–350. <https://doi.org/10.1007/s00427-013-0449-5>
- Scheer, N., Campos-Ortega, J.A., 1999. Use of the Gal4-UAS technique for targeted gene expression in the zebrafish. *Mech. Dev.* 80, 153–158. [https://doi.org/10.1016/s0925-4773\(98\)00209-3](https://doi.org/10.1016/s0925-4773(98)00209-3)
- Schinko, J.B., Weber, M., Viktorinova, I., Kiupakis, A., Averof, M., Klingler, M., Wimmer, E.A., Bucher, G., 2010. Functionality of the GAL4/UAS system in *Tribolium* requires the use of endogenous core promoters. *BMC Dev. Biol.* 10, 53. <https://doi.org/10.1186/1471-213X-10-53>
- Schlipalius, D.I., Chen, W., Collins, P.J., Nguyen, T., Reilly, P.E.B., Ebert, P.R., 2008. Gene interactions constrain the course of evolution of phosphine resistance in the lesser grain borer, *Rhyzopertha dominica*. *Heredity* 100, 506–516. <https://doi.org/10.1038/hdy.2008.4>
- Schlipalius, D.I., Cheng, Q., Reilly, P.E.B., Collins, P.J., Ebert, P.R., 2002. Genetic linkage analysis of the lesser grain borer *Rhyzopertha dominica* identifies two loci that confer high-level resistance to the fumigant phosphine. *Genetics* 161, 773–782. <https://doi.org/10.1093/genetics/161.2.773>
- Schlipalius, D.I., Tuck, A.G., Jagadeesan, R., Nguyen, T., Kaur, R., Subramanian, S., Barrero, R., Nayak, M., Ebert, P.R., 2018. Variant Linkage Analysis Using de Novo Transcriptome Sequencing Identifies a Conserved Phosphine Resistance Gene in Insects. *Genetics* 209, 281–290. <https://doi.org/10.1534/genetics.118.300688>
- Schlipalius, D.I., Valmas, N., Tuck, A.G., Jagadeesan, R., Ma, L., Kaur, R., Goldinger, A., Anderson, C., Kuang, J., Zuryn, S., Mau, Y.S., Cheng, Q., Collins, P.J., Nayak, M.K., Schirra, H.J., Hilliard, M.A., Ebert, P.R., 2012. A core metabolic enzyme mediates resistance to phosphine gas. *Science* 338, 807–810. <https://doi.org/10.1126/science.1224951>
- Schmidt-Ott, U., Lynch, J.A., 2016. Emerging developmental genetic model systems in holometabolous insects. *Curr. Opin. Genet. Dev.* 39, 116–128. <https://doi.org/10.1016/j.gde.2016.06.004>
- Schröder, R., Beermann, A., Wittkopp, N., Lutz, R., 2008. From development to biodiversity—*Tribolium castaneum*, an insect model organism for short germband development. *Dev. Genes Evol.* 218, 119–126. <https://doi.org/10.1007/s00427-008-0214-3>
- Sharma, P., Yan, F., Doronina, V.A., Escuin-Ordinas, H., Ryan, M.D., Brown, J.D., 2012. 2A peptides provide distinct solutions to driving stop-carry on translational recoding. *Nucleic Acids Res.* 40, 3143–3151. <https://doi.org/10.1093/nar/gkr1176>

- Shirai, Y., Piulachs, M.-D., Belles, X., Daimon, T., 2022. DIPA-CRISPR is a simple and accessible method for insect gene editing. *Cell Rep. Methods* 2, 100215.
<https://doi.org/10.1016/j.crmeth.2022.100215>
- Shukla, J.N., Palli, S.R., 2012. Sex determination in beetles: Production of all male progeny by Parental RNAi knockdown of transformer. *Sci. Rep.* 2, 602. <https://doi.org/10.1038/srep00602>
- Smirnikhina, S.A., 2020. Prime Editing: Making the Move to Prime Time. *CRISPR J.* 3, 319–321.
<https://doi.org/10.1089/crispr.2020.29105.sas>
- Stamatakis, E., Pavlopoulos, A., 2016. Non-insect crustacean models in developmental genetics including an encomium to *Parhyale hawaiiensis*. *Curr. Opin. Genet. Dev., Developmental mechanisms, patterning and evolution* 39, 149–156. <https://doi.org/10.1016/j.gde.2016.07.004>
- Stern, C. (Ed.), 2004. *Gastrulation: From Cells to Embryo*, 1st edition. ed. Cold Spring Harbor Laboratory Press, Cold Spring Harbor, N.Y.
- Szybalski, W., Kim, S.C., Hasan, N., Podhajski, A.J., 1991. Class-II restriction enzymes — a review. *Gene* 100, 13–26. [https://doi.org/10.1016/0378-1119\(91\)90345-C](https://doi.org/10.1016/0378-1119(91)90345-C)
- Traven, A., Jelacic, B., Sopta, M., 2006. Yeast Gal4: a transcriptional paradigm revisited. *EMBO Rep.* 7, 496–499. <https://doi.org/10.1038/sj.embor.7400679>
- Trevino, A.E., Zhang, F., 2014. Chapter Eight - Genome Editing Using Cas9 Nickases, in: Doudna, J.A., Sontheimer, E.J. (Eds.), *Methods in Enzymology, The Use of CRISPR/Cas9, ZFNs, and TALENs in Generating Site-Specific Genome Alterations*. Academic Press, pp. 161–174.
<https://doi.org/10.1016/B978-0-12-801185-0.00008-8>
- Valmas, N., Zuryn, S., Ebert, P.R., 2008. Mitochondrial uncouplers act synergistically with the fumigant phosphine to disrupt mitochondrial membrane potential and cause cell death. *Toxicology* 252, 33–39. <https://doi.org/10.1016/j.tox.2008.07.060>
- van Soolingen, D., de Haas, P.E., Hermans, P.W., Groenen, P.M., van Embden, J.D., 1993. Comparison of various repetitive DNA elements as genetic markers for strain differentiation and epidemiology of *Mycobacterium tuberculosis*. *J. Clin. Microbiol.* 31, 1987–1995.
<https://doi.org/10.1128/jcm.31.8.1987-1995.1993>
- Viktorinová, I., Wimmer, E.A., 2007. Comparative analysis of binary expression systems for directed gene expression in transgenic insects. *Insect Biochem. Mol. Biol.* 37, 246–254.
<https://doi.org/10.1016/j.ibmb.2006.11.010>
- Watakabe, I., Hashimoto, H., Kimura, Y., Yokoi, S., Naruse, K., Higashijima, S., 2018. Highly efficient generation of knock-in transgenic medaka by CRISPR/Cas9-mediated genome engineering. *Zool. Lett.* 4, 3. <https://doi.org/10.1186/s40851-017-0086-3>
- Watson, J.D., 2014. *Molecular Biology of the Gene*. Pearson.
- Webster, N., Jin, J.R., Green, S., Hollis, M., Chambon, P., 1988. The yeast UASG is a transcriptional enhancer in human HeLa cells in the presence of the GAL4 trans-activator. *Cell* 52, 169–178.
[https://doi.org/10.1016/0092-8674\(88\)90505-3](https://doi.org/10.1016/0092-8674(88)90505-3)
- Wu, C., Chakrabarty, S., Jin, M., Liu, K., Xiao, Y., 2019. Insect ATP-Binding Cassette (ABC) Transporters: Roles in Xenobiotic Detoxification and Bt Insecticidal Activity. *Int. J. Mol. Sci.* 20, 2829.
<https://doi.org/10.3390/ijms20112829>
- Zhang, J., Yin, Z., White, F., 2015. TAL effectors and the executor R genes. *Front. Plant Sci.* 6.
- Zuo, Y., Wang, H., Xu, Y., Huang, J., Wu, S., Wu, Y., Yang, Y., 2017. CRISPR/Cas9 mediated G4946E substitution in the ryanodine receptor of *Spodoptera exigua* confers high levels of resistance to diamide insecticides. *Insect Biochem. Mol. Biol.* 89, 79–85.
<https://doi.org/10.1016/j.ibmb.2017.09.005>